MAP0006: D5.6 Epithermal testing report.

01 December 2020

KAVA Reference (17034, MAP, Mineral Resource Assessment Platform):

Name of the author/Responsible partner: Tobias Björn Weisenberger, Gunnlaugur M Einarsson, Albert Þorbergsson, Iceland GeoSurvey (ÍSOR), Reykjavík, Iceland

Version No: 02

This activity has received funding from the European Institute of Innovation and Technology (EIT), a body of the European Union, under the Horizon 2020, the EU Framework Programme for Research and Innovation

Content

This activity has received funding from the European Institute of Innovation and Technology (EIT), a body of the European Union, under the Horizon 2020, the EU Framework Programme for Research and Innovation

Abstract

Hydrothermal system within Iceland are prone for mobilization of metals that can lead to the enrichment of metals and eventually can form a mineral deposit. In order to evaluate undiscovered resource of gold in epithermal systems in Iceland a three-part assessment was conducted. The assessment was carried out by using the software tool MAPWizard that was develop with the EIT Raw Material funded project Mineral Resource Assessment Platform (MAP). The reports included information on the model of epithermal gold formation in Iceland. A recent USGS Grade-tonnage model for epithermal gold (-silver) deposits have been adapted. Within an assessment workshop, experts estimated undiscovered deposits within three selected permissive tracts that based on the model of central volcanoes in Iceland. Using the MAPWizard the probability of undiscovered gold in the selected permissive tracts were assessed and are presented in this report.

The Breiðdalur tract covers an area of 83 km^2. The expected number of undiscovered deposits within the delineated permissive tracts is 0.135 (mean estimate), and the undiscovered deposits are estimated to contain, with 50% probability, no gold. For a probability of 10%, it contains at least 1.45 t of gold. The Hafnarfjall tract covers an area of 222 km^2. The expected number of undiscovered deposits within the delineated permissive tracts is 0.134 (mean estimate), and the undiscovered deposits are estimated to contain, with 50% probability, no gold. For a probability of 10%, it contains at least 1.37 t of gold. The Kjarlanes/Stardalur tract covers an area of 270 km^2. The expected number of undiscovered deposits within the delineated permissive tracts is 0.778 (mean estimate), and the undiscovered deposits are estimated to contain, with 50% probability, contains at least 0.35 t of gold. For a probability of 10%, it contains at least 129 t of gold.

1. Introduction

Mineral Resource Assessment Platform (MAP) is an EIT RawMaterials Upscaling project. The project started 1 January 2018, and its duration is three years. The project is funded by EIT RawMaterials. There are eight partners in the consortium.
The project produced an enhanced and upgraded method and software for the quantitative assessment of undiscovered mineral resources, by integrating mineral perspectivity modelling and the three-part method. The testing phase of the software produced valuable information on undiscovered resources in the Nordic countries and Germany, and on the Arctic deep ocean floor. The MAP software will increase the productivity of its users and create new business possibilities for service providers.
This report presented the three-part assessment of undiscovered epithermal gold in Iceland. After the introduction chapter 2 provides an overview of the three-part resource assessment method. Chapter 3 provides more detailed information on the three-part quantitative resource assessment method. Within chapter 4 the general information on epithermal gold deposits are presented. Chapter 5 gives an overview of the geology of Iceland and detailed information on epithermal gold, including information on the exploration history, gold prospects as well as an ore formation model. Chapter 6 is dedicated the assessment of epithermal gold in Iceland by using the MAP Wizard. Chapter 7 provides a summary.

2. The three-part resource assessment

The procedure we selected is based on a three-part quantitative assessment method developed at the USGS starting from the mid-1970s (Singer, 1975; Singer and Menzie 2010 Kaveli at al., 2014 and reference therein).

Selection or development of a **deposit model**
• Characterize the mineral deposit type being assessed

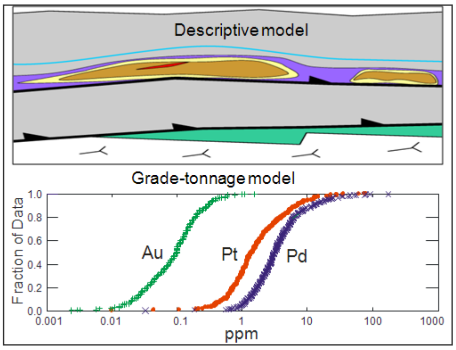

This activity has received funding from the European Institute of Innovation and Technology (EIT), a body of the European Union, under the Horizon 2020, the EU Framework Programme for Research and Innovation

Delineation of **permissive tracts**

- Areas where the deposit type can exist

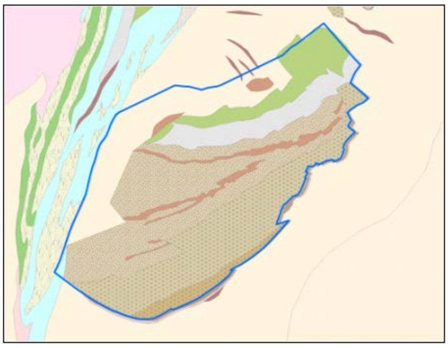

Estimation of **number of undiscovered deposits**

- Within the permissive tracts

	Number of deposits at the indicated probability		
	90 %	50 %	10 %
	2	4	5
	2	4	6
	2	3	5
Consensus / Average	**2**	**4**	**5**

Figure 1. Component of the he three-part method (courtesy. Kalevi Rasilainen, GTK).

The assessment is based on statistical methods of data analysis and integration and it treats and expresses uncertainty. The method enables the use of varying amounts of objective geological data and subjective expert knowledge, and it generates reproducible assessment results.
The three-part method consists of the following components (Figure 1):
(1) evaluation and selection or construction of descriptive models and grade-tonnage models for the deposit types under consideration,
(2) delineation of areas according to the types of deposits permitted by the geology (permissive tracts), and
(3) estimation of the number of undiscovered deposits of each deposit type within the permissive tracts. The estimated number of deposits is combined with the grade and tonnage distributions from the deposit models to assess the total undiscovered metal endowment.

This activity has received funding from the European Institute of Innovation and Technology (EIT), a body of the European Union, under the Horizon 2020, the EU Framework Programme for Research and Innovation

3. The three-part quantitative resource assessment method

3.1. Descriptions and definitions of the modules

The following descriptions are mainly adopted from Rasilainen et al. (2014).
Deposit models designed for quantitative assessments are the cornerstone of the method. They are used to classify mineralized and barren environments, as well as types of known deposits, and to discriminate mineral deposits from mineral occurrences (Singer and Berger 2007). Deposit models that can be used in the three-part assessment method include descriptive models, grade-tonnage models, deposit density models, economic models and quantitative descriptive models. Descriptive models and grade-tonnage models are an essential component of the three-part method.

Descriptive model

A descriptive model consists of systematically arranged information describing the essential characteristics of mineral deposits of the class to be assessed (Barton, 1993). A descriptive model usually consists of two parts. The first part describes the geological environments in which the deposits occur. It contains information on favorable host rocks, possible source rocks, age ranges of mineralization, the depositional environment, tectonic setting, and associated deposit types. This part of the descriptive model plays a crucial role in the delineation of permissive tracts, i.e., areas where the geology permits the occurrence of deposits of the type under consideration. The second part of a descriptive model lists the essential identifying characteristics by which a given deposit type might be recognized. These include ore textures and structures, mineralogy, alteration, and geochemical and geophysical signatures. The second part of the model is used to classify known deposits and occurrences. Identifying the types of known deposits is important for the tract delineation process, and it can sometimes help to delineate geological environments not indicated on geological maps.

Grade-tonnage model

A grade-tonnage model consists of data on average metal grades and the associated total tonnage of well-studied and completely delineated deposits of a certain type (Singer 1993; Singer

This activity has received funding from the European Institute of Innovation and Technology (EIT), a body of the European Union, under the Horizon 2020, the EU Framework Programme for Research and Innovation

and Menzie, 2010). The total tonnage combines total past production and current resources (including reserves) at the lowest possible cut-off grade. Grade-tonnage models are usually presented as frequency distributions of tonnage and average metal grades. These distributions are used as models for grades and tonnages of undiscovered deposits of the same type in geologically similar settings. They also help in differentiating between a deposit and a mineral occurrence, and in judging whether a deposit or group of deposits belongs to the type represented by the model.

It is very important to use the same sampling unit criteria for all deposits in the grade-tonnage model. Mixing old production data from some deposits with resource data from other deposits is among the most common errors in the construction of grade-tonnage models and will produce biased models (Singer and Berger, 2007). Spatial aspects of the sampling unit must also be considered. A spatial rule identifying the minimum distance between two separate deposits of a given type should be defined and deposits closer to each other than the minimum distance should be combined in the grade-tonnage model.

Permissive tract

A permissive tract is an area within which the geology permits the existence of mineral deposits of the type under consideration (Singer, 1993; Singer and Menzie, 2010). It is important to distinguish between areas favorable for the existence of deposits and permissive tracts: the former are subsets of the latter. The existence of a permissive tract in an area does not indicate any favorability for the occurrence of deposits within the area; neither has it anything to do with the likelihood of discovery of existing undiscovered deposits in the area.

In the three-part assessment method, permissive tracts should be based on criteria derived from descriptive models. Tract boundaries should be defined so that the likelihood of deposits occurring outside of the tract is negligible. The boundaries of the tracts are first defined based on mapped or inferred geology. Tracts may or may not contain known deposits. The existence of deposits is used to confirm and extend the tracts, but the lack of known deposits is not a reason to exclude any part of a permissive area from the tract. Original tract boundaries should only be reduced where it can be firmly demonstrated that a deposit type could not exist. This evidence could be based on geology, knowledge of unsuccessful exploration, or the presence of barren overburden exceeding the predetermined delineation depth limit.

Undiscovered deposits

The third part of the three-part assessment method is the estimation of the number of undiscovered deposits of the type(s) that may exist in the delineated tracts (Singer, 1993; Singer and Menzie, 2010). The estimates represent the probability that a certain fixed but unknown

This activity has received funding from the European Institute of Innovation and Technology (EIT), a body of the European Union, under the Horizon 2020, the EU Framework Programme for Research and Innovation

number of undiscovered deposits exist in the delineated tracts. The estimates are carried out according to deposit type and they must be consistent with the grade-tonnage models. This means that, for example, about half of the estimated undiscovered deposits should be larger than the median tonnage given by the grade-tonnage model and about 10% of the estimated deposits should be larger than the upper 10th quantile of the model. The spatial rule used to define a deposit in the grade-tonnage model must be respected in the estimates. Well-explored and completely delineated deposits, for which published grade and tonnage values exist, are considered as discovered deposits, whereas deposits without publicly available grade and tonnage information, partly delineated deposits, and known occurrences without reliable grade-tonnage estimates are counted as undiscovered.

Several methods can be used either directly or as guidelines to make the estimates. These include the frequency of deposits in well-explored geologically analogous areas (deposit density models), local deposit extrapolations, counting and assigning probabilities to geophysical and/or geochemical anomalies, process constraints, relative frequencies of associated deposit types, and limits set by the total available area or total known metal (Singer, 2007). Some of these methods produce a single estimate of the expected number of deposits; others produce a probability distribution of the expected number of deposits. In the latter case, the spread of the estimates for the number of deposits associated with high and low quantiles of the probability distribution (for example, the 90 % and 10 % quantiles) indicates the uncertainty of the estimate. The expected number of deposits, or the estimated number of deposits associated with a given probability level, measures the likelihood of the existence of a deposit type.

The estimates are typically made subjectively by a team of experts knowledgeable about the deposit type and the geology of the region. The process follows the Delphi technique (Chorlton et al., 2007), in which each expert makes an estimate independently and all the estimates are then discussed to possibly reach a final consensus estimate.

Statistical evaluation - Monte Carlo simulation

The three parts of the assessment method described above produce consistent estimates of the number of undiscovered deposits for the delineated areas and of the probability distribution of grades and tonnages of the deposit type (Singer and Menzie, 2010). As the final step of the assessment, these estimates are combined using statistical methods to achieve probability distributions of the quantities of contained metals and ore tonnages in the undiscovered deposits. Software using Monte Carlo simulation has been developed for this purpose (Root et al., 1992; Duval, 2012), and is implemented in the MAP software.

This activity has received funding from the European Institute of Innovation and Technology (EIT), a body of the European Union, under the Horizon 2020, the EU Framework Programme for Research and Innovation

3.2. Terminology

Some terms essential to the proper understanding of this report are briefly described below. The definitions follow the usage by the minerals industry and the resource assessment community (U.S. Bureau of Mines and U.S. Geological Survey 1980, U.S. Geological Survey National Mineral Resource Assessment Team 2000, Committee for Mineral Reserves International Reporting Standards 2013).

Mineral deposit

A mineral occurrence of sufficient size and grade that it might, under the most favorable circumstances, be considered to have economic potential.

Well-known mineral deposit

A completely delineated mineral deposit, for which the identified resources and past production ore known.

Undiscovered mineral deposit

A mineral deposit believed to exist less than 1 km below the surface of the ground, or an incompletely explored mineral occurrence within that depth range that could have sufficient size and grade to be classified as a deposit.

Mineral occurrence

A concentration of any useful mineral found in bedrock in sufficient quantity to suggest further exploration.

Mineral resource

A concentration or occurrence of material of economic interest in or on the Earth's crust in such a form, quality and quantity that there are reasonable prospects for eventual economic extraction. The location, quantity, grade, continuity and other geological characteristics of a mineral resource are known, estimated or interpreted from specific geological evidence, sampling and knowledge.

This activity has received funding from the European Institute of Innovation and Technology (EIT), a body of the European Union, under the Horizon 2020, the EU Framework Programme for Research and Innovation

Identified resources

Resources whose location, grade, quality and quantity are known or can be estimated from specific geological evidence.

Well-known resources

Identified resources that occur in completely delineated deposits included in grade-tonnage models.

Discovered resources

The total amount of identified resources and cumulative past production.

Undiscovered resources

Resources in undiscovered mineral deposits whose existence is postulated based on indirect geological evidence.

Hypothetical resources

Undiscovered resources in known types of mineral deposits postulated to exist in favorable geological settings where other well-explored deposits of the same types are known.

Speculative resources

Undiscovered resources that may occur either in known types of deposits in favorable geological settings where mineral discoveries have not been made, or in types of deposits as yet unrecognized for their economic potential.

This activity has received funding from the European Institute of Innovation and Technology (EIT), a body of the European Union, under the Horizon 2020, the EU Framework Programme for Research and Innovation

4. Epithermal gold deposits

Epithermal descriptive model is adapted from John et al. (2018).

4.1. Definition and classification of epithermal gold deposits

The term "epithermal" was originally applied by Lindgren (1928, 1933) to mineral deposits mined primarily for gold, silver, mercury, antimony, and base metals (Cu, Pb, and Zn), and deposited "at slight depth below the surface," at temperatures "perhaps from 50 to 200 °C," and at pressures that "scarcely exceed 100 atmospheres." Since Lindgren's seminal studies, it has been recognized that epithermal deposits form at temperatures as high as about 300 °C and at depths from about 50 to as much as 1,500 m below the water table, and that these deposits commonly represent the shallow parts of larger, mainly subaerial, hydrothermal systems (Figure 2; Henley and Ellis, 1983; Cooke and Simmons, 2000; Simmons et al., 2005).

As summarized by Simmons et al. (2005), all modern classification systems consider ore or gangue mineralogy features, and many use chemical characteristics (pH, oxidation state, or sulfidation state) of fluids associated with proximal hydrothermal alteration and (or) ore mineralization. The large number of proposed classification schemes reflects the wide range of characteristic features displayed by these deposits and the evolution in thinking about their origins.

The model presented here is restricted to deposits that fit the expanded definition of epithermal, and were, or are, mined because of their gold content. As a group, epithermal gold deposits have common and distinctive characteristics. Broadly common characteristics include tectonic setting, host rocks, deposit forms, ages, and temperatures and depths of formation, whereas ore, gangue, and alteration mineral assemblages and zoning, ore-fluid chemistry, and sources of deposit components vary considerably among deposits. Especially noteworthy are differences in sulfide mineral assemblages that reflect differences in the sulfidation state of inferred ore-fluid chemistry (Figure 3, Table 1; Hedenquist et al., 2000; Einaudi et al., 2003; Sillitoe and Hedenquist, 2003). The three deposit subtypes included in this model, high-, intermediate-, and low-sulfidation, are named to reflect differences in the sulfur fugacity of ore fluids that form major sulfide mineral assemblages (solid red lines, Figure 3).

This activity has received funding from the European Institute of Innovation and Technology (EIT), a body of the European Union, under the Horizon 2020, the EU Framework Programme for Research and Innovation

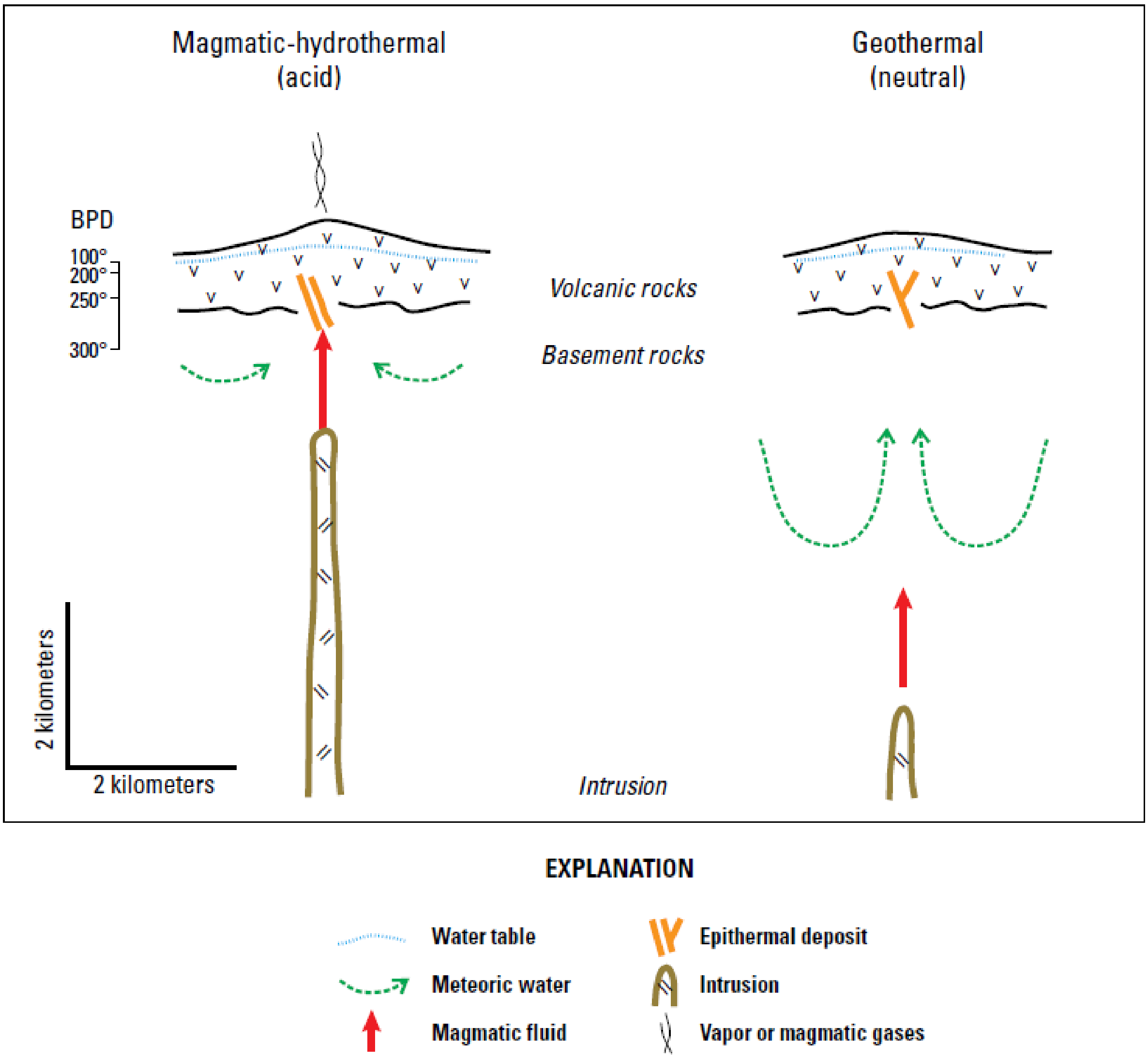

Figure 2. Schematic cross sections showing end-member magmatic-hydrothermal and geothermal systems and positions of low-sulfidation (neutral) and high-sulfidation (acid) epithermal environments within these systems. The maximum pressure-temperature gradient under hydrostatic conditions is represented by boiling point for depth (BPD). Adapted from John et al. (2018), which was redrawn from Simmons et al. (2005).

This activity has received funding from the European Institute of Innovation and Technology (EIT), a body of the European Union, under the Horizon 2020, the EU Framework Programme for Research and Innovation

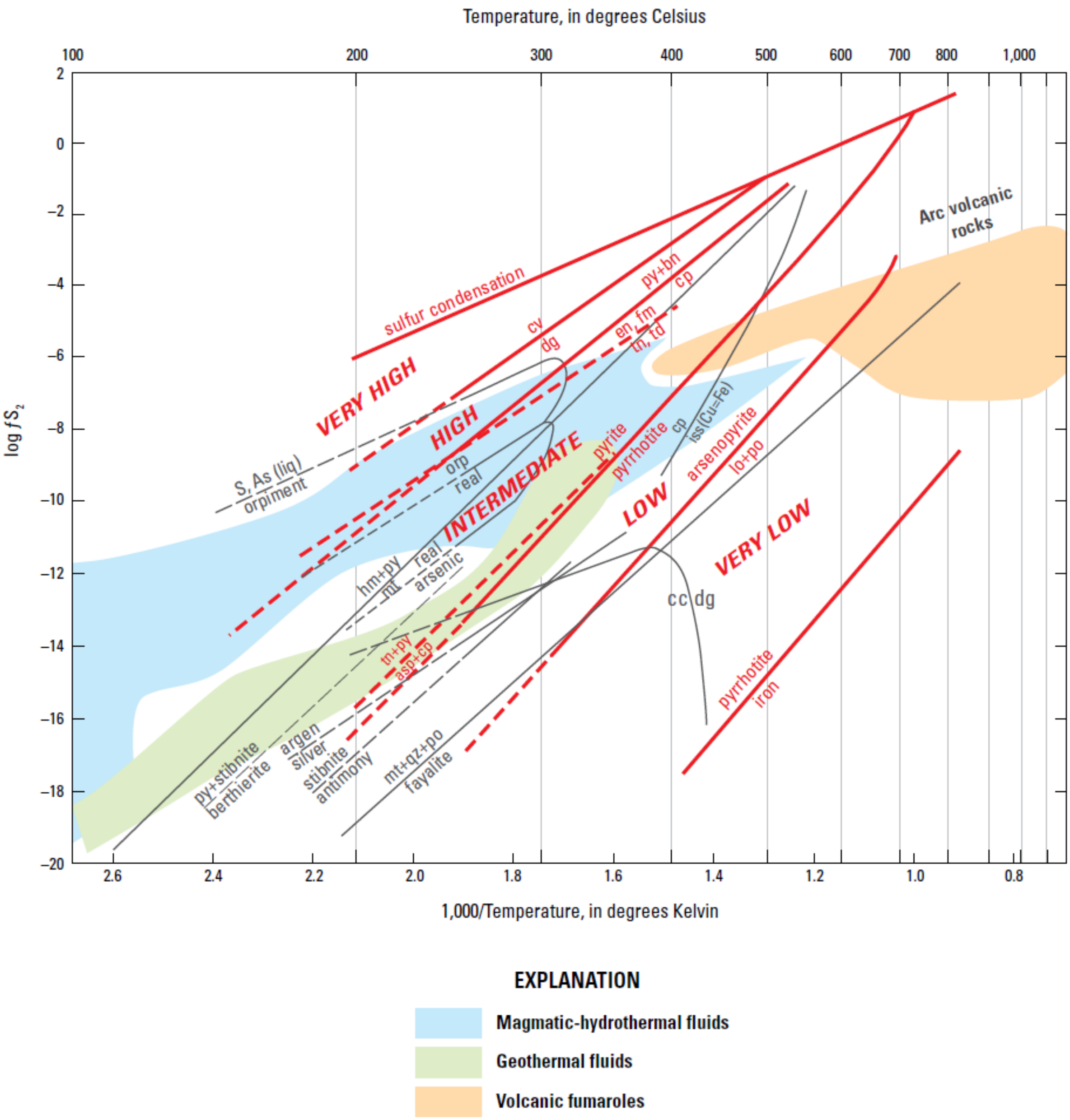

Figure 3. Sulfur fugacity (fS_2)-temperature diagram showing the variety of sulfide assemblages in epithermal deposits that reflect sulfidation state, from very low and low through intermediate to high and very high. Thick red lines represent boundaries between these sulfidation states. Compositional fields of arc volcanic rocks, high-temperature volcanic fumaroles, magmatic-hydrothermal fluids, and geothermal fluids also are shown, as discussed by Einaudi et al. (2003). Figure modified from Sillitoe and Hedenquist (2003). Element and mineral abbreviations: As, arsenic; argen, argentite; cc, chalcocite; Cu, copper; dg, digenite; Fe, iron; hm, hematite; iss, intermediate solid solution; lo, loellingite; mt, magnetite; orp, orpiment; qz, quartz; real, realgar; S, sulfur.

This activity has received funding from the European Institute of Innovation and Technology (EIT), a body of the European Union, under the Horizon 2020, the EU Framework Programme for Research and Innovation

Table 1. Characteristics of epithermal gold deposit subtypes and variants.

[Ag, silver; Au, gold; As, arsenic; Bi, bismuth; equiv., equivalent; Fe, iron; Hg, mercury; m, meters; Mn, manganese; Te, tellurium; Sb, antimony; Se, selenium; Sn, tin; vol., volume; %, percent]

	High-sulfidation	Low-sulfidation	Intermediate-sulfidation
Spatially and temporally associated volcanic rocks	Calc-alkaline, andesite-dacite	Calc-alkaline, andesite-rhyolite; tholeiitic, bimodal basalt-rhyolite	Calc-alkaline, andesite-rhyolite
Volcanic landforms and deposits	Lava domes and flows, diatremes, tuff rings, maars, and intrusive breccias associated with diatremes; uplands and basins of pyroclastic and volcaniclastic rocks	Lava domes and flows; uplands and basins of pyroclastic and volcaniclastic rocks; dikes	Lava domes and flows, diatremes, tuff rings, maars, and intrusive breccias associated with diatremes; uplands and basins of pyroclastic and volcaniclastic rocks
Tectonic setting (table E1)	Compressional-transpressional continental-margin arc or back arc; compressional-transpressional, neutral stress to mildly extensional continental-margin arc	Extensional continental-margin and island arcs; extensional back arc; post-arc continental extension	Extensional continental-margin arc; compressional island arc; continental rift
Proximal alteration minerals	Alunite, kaolinite (dickite), pyrite, pyrophyllite, residual, vuggy quartz, aluminum-phosphate-sulfate (APS) minerals	Quartz-adularia±illite±pyrite	Quartz+adularia+illite+pyrite
Silica and carbonate gangue and textural features	Structurally and stratigraphically controlled fine-grained silicification and residual, vuggy quartz; no carbonate minerals	Vein-filling crustiform and colloform chalcedony and quartz; minor late calcite and (or) calcite-replacement texture	Fault zone replacement and vein-filling by fine- to coarse-grained equigranular quartz, and crustiform and comb quartz; calcite late or distal to thermal centers
Other gangue	Minor barite common, typically late	Barite uncommon; fluorite present locally	Barite and manganiferous silicates present locally
Gold-silver and other ore minerals	Gold, electrum, Au-Ag tellurides, acanthite, Ag-bearing tennantite, tetrahedrite, enargite, luzonite, chalcopyrite	Electrum, Ag sulfides, selenides and sulfosalts; low Ag/Au; generally no other metals recovered	Electrum, Ag sulfides and sulfosalts; high Ag/Au; chalcopyrite, galena, sphalerite
Sulfide abundance	5 to 90 vol. %	Typically <1 to 2 vol. % except where hosted by basalts (as much as 20 vol. %)	5 to >20 vol. %
Sulfide minerals	Pyrite, enargite, luzonite, covellite-digenite, famatinite, chalcopyrite, tetrahedrite/tennantite, Fe-poor sphalerite	Pyrite/marcasite, Au-Ag sulfides/sulfosalts, arsenopyrite, pyrrhotite, Fe-poor to Fe-rich sphalerite, cinnabar, stibnite	Pyrite, Au-Ag sulfides/sulfosalts, Fe-poor sphalerite, galena, chalcopyrite, tetrahedrite/tennantite
Other enriched metals	As, Sb, Bi, Sn, Te, Se	As, Sb, Se, Hg	Mn, Se
Te and Se minerals	Au-Ag tellurides common; selenides present locally	Au-Ag selenides, Se sulfosalts common	Tellurides common locally; selenides uncommon
Deposit style, veins, and mineralized structures	Breccias; diatremes; residual vuggy quartz; stratabound disseminated; massive sulfide; veins and stockworks; veins generally late	Multiple stage veins of fine concordant and discordant layered mineral assemblages and breccias, comb and crustiform textures; sheeted veins; vein stockworks and breccias; fault intersections; disseminated	Multistage veins and associated breccias with coarse layers and comb and crustiform textures; disseminated; diatremes
Paleosurface indicators	Steam-heated blankets over some deposits	Sinter and explosion breccias; chalcedony blankets; steam-heated blankets over some deposits; thin quartz veins and stockworks over some deposits	Rarely documented; thin quartz veins and stockworks over some deposits
Depth to top of ore zones (meters below water table)	Tens of meters to 700 m	Meters to several hundred meters	Several hundred meters
Vertical extent of ore	100 to 800 m	Mostly 100 to 400 m	Up to ~1,000 m
Fluid inclusion homogenization temperature and composition	Mostly 155 to 330 °C (220 to 270 °C modes); ~0–6 weight % NaCl equiv.; halide saturated fluids in some deposits	<100 to 390 °C (<130 to 290 °C modes); 0 to 6 weight % NaCl equiv. (mostly <3%)	135 to 385 °C (220 to 310 °C modes); as much as 23 weight % NaCl equiv. (mostly 1 to 12%)
Representative deposits	Yanacocha, Pueblo Viejo, Pierina, Pascua-Lama, Goldfield, Summitville	Hishikari, Midas, Sleeper, McLaughlin, National, Mule Canyon	Comstock Lode, Tonopah, Fresnillo, El Peñón, Waihi, Peñasquito, Roşia Montană

This activity has received funding from the European Institute of Innovation and Technology (EIT), a body of the European Union, under the Horizon 2020, the EU Framework Programme for Research and Innovation

4.2. General characteristic of epithermal Au (Ag) deposits

Epithermal deposits form in the upper crust at the paleosurface to depths about 1,500 m below the water table and at temperatures that range from about 100 to 300 °C. Most deposits are genetically related to hydrothermal systems associated with subaerial volcanism and intrusion of subduction-related calc-alkaline magmas ranging in composition from basalt to rhyolite in island- and continental-arc settings; less commonly, these deposits are related to hydrothermal systems associated with continental rifting or hot spot magmatism. Lava dome and associated diatreme complexes are the volcanic features most commonly temporally and spatially associated with ore formation and host many epithermal deposits; less common volcanic hosts include stratovolcanoes, ignimbrite calderas, and dike complexes. Most epithermal deposits are related to hydrothermal systems that form in response to release of magmatic fluids (degassing) from crystallizing intrusions at depth.

Epithermal gold-silver deposits form in a variety of tectonic settings that range from extensional to transtensional, transpressional, and compressional. Within this broad range of regional tectonic settings, epithermal deposits most commonly occur as veins or breccias developed in local extensional or dilational fault and fracture zones. Disseminated and replacement ore also commonly forms in permeable lithologies where horizons intersect faults or fractures that allowed fluid ingress.

The character of hydrothermal alteration associated with epithermal deposits varies considerably between deposit subtypes, and within deposits, as a consequence of varying spatial relations with the paleowater table. High-sulfidation deposits are characterized by a core zone of residual (vuggy) quartz flanked by quartz-alunite and advanced argillic alteration containing kaolinite/dickite and (or) pyrophyllite produced by very low pH fluids below the paleowater table. In contrast, potassic alteration with quartz, adularia and (or) carbonate minerals and (or) illite, indicative of formation from near-neutral pH fluids, forms the core of low- and intermediate-sulfidation deposits. More distal argillic and propylitic alteration may fringe all deposit subtypes. Above the paleowater table, steam-heated advanced argillic and argillic alteration assemblages composed of alunite, kaolinite, smectite, and cristobalite or opaline silica may form in association with all deposit subtypes. Silica sinter deposits are present near and locally host some low-sulfidation deposits but are absent in high-sulfidation deposits.

Distinct ore and gangue mineral assemblages characterize each of the deposit subtypes. Ore minerals in low-sulfidation deposits include electrum, silver sulfides, selenides, and sulfosalts, and (or) gold and silver tellurides, and in intermediate-sulfidation deposits, base metal sulfides, including silver-bearing tetrahedrite-tennantite, chalcopyrite, galena, and sphalerite, also may be present. Gangue minerals in these deposits include quartz, adularia, illite/sericite, and carbonate minerals. Gold and (or) electrum, gold tellurides, acanthite, enargite, luzonite, and other copper

sulfide and sulfosalt minerals, hosted by quartz gangue, characterize high-sulfidation deposits. Pyrite and (or) marcasite are common in all deposit subtypes.
Epithermal gold-silver deposits commonly contain elevated abundances of As, Sb, Hg, Se, Te, Tl, and (or) W; some deposits also are enriched in Pb, Zn, Cu, and Mo. However, concentrations of these elements (ppm to weight percent) varies widely within individual deposits, between different deposits within each subtype of deposit, and between each deposit subtype; commonly gold abundance is the best indicator of gold mineralization.
Stable and radiogenic isotope and fluid inclusion studies of epithermal deposits indicate that meteoric waters, containing variable magmatic volatile contents, are principally responsible for gold-silver mineralization. High-sulfidation deposits typically have isotopic compositions consistent with larger magmatic fluid contributions than in low- and intermediate-sulfidation deposits. The ultimate origin of gold, silver, and other metals in epithermal gold-silver deposits remains uncertain but probably reflects multiple sources in the upper mantle and crust.

5. Epithermal gold in Iceland

5.1. General geology of Iceland

Iceland is located in the North Atlantic Ocean between Greenland and Norway at 63°2´´N to 66°30´´N. It is a landmass that is part of a much larger entity situated at the junction of two large submarine physiographic structures, the Mid-Atlantic Ridge and the Greenland-Iceland-Faeroe Ridge (Figure 4). As such, Iceland is a part of the oceanic crust forming the floor of the Atlantic Ocean and is the subaerial part of the Iceland Basalt Plateau, which rises more than 3000 m above the surrounding sea floor and covers about 350,000 km^2. About 30 per cent of the plateau (~103,000 km^2) is above sea level, the remainder forms the 50 – 200 km wide shelf around the island, sloping gently to depths of ~400 m before cascading into the abyss.
Iceland is geologically very young, and all of its rocks were formed within the last 25 million years. The stratigraphic succession of Iceland extends across two geological periods: The Tertiary and the Quaternary (Table 2). The construction of the Iceland is thought to have begun about 24 million years ago, but the oldest rocks exposed at the surface in Iceland are only 14 - 16 million years old. If we take the age of the Earth as one year, then Iceland was born less than two days ago. The first regional glaciers of the Ice Age appeared in Iceland about five hours ago and only a minute has passed since the Holocene warming removed this ice cover from Iceland.

This activity has received funding from the European Institute of Innovation and Technology (EIT), a body of the European Union, under the Horizon 2020, the EU Framework Programme for Research and Innovation

The surface of Iceland has changed radically during its brief existence by construction (i.e. volcanism and sedimentation) and degradation (i.e. erosion). These forces of nature operate faster in Iceland than in most other places. The rocks are shattered by the frequent change of frost to thaw, and the sea, rivers and glaciers laboriously grind down the land. Erosion removes about a million cubic meters of land from Iceland each year, but volcanism and sedimentation more than counterbalance this loss as is evident in the landmass that now is Iceland.

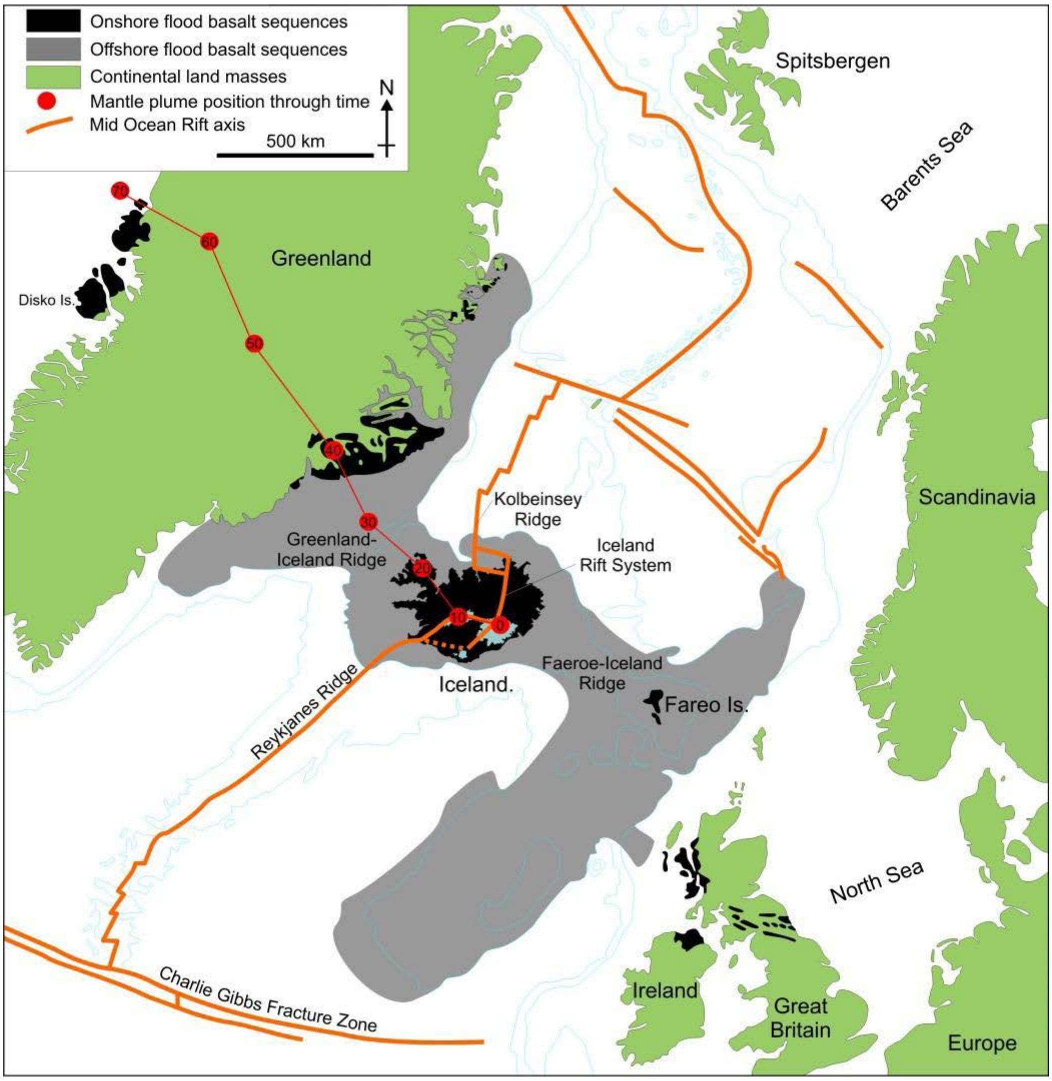

Figure 4. Iceland is an elevated plateau in the middle of the North Atlantic, situated at the junction between the Reykjanes and Kolbeinsey Ridge segments. Also shown: the axis of the Mid-Atlantic Ridge (heavy solid line), the North Atlantic basalt plateau (black) and their submarine equivalents (grey). The line with the dots shows the position of the Iceland mantle plume from 65 million years to the present day (taken from Thordarson, 2012).

This activity has received funding from the European Institute of Innovation and Technology (EIT), a body of the European Union, under the Horizon 2020, the EU Framework Programme for Research and Innovation

Table 2. Geologic timetable for Iceland showing the terminology used in this text for geologic periods, epochs and stages. Age is shown in thousands (ky) or millions (my) years (taken from Thordarson, 2012).

Era	Period	Epoch	Age	Stage	Sub-Stage	Formations	Events
Cainozoic	Quaternary	Holocene	0 2.5ky	Late Bog Period (sub-Atlantic)		Upper Pleistocene Formation	
			5.0ky	Late Birch Period (sub Boreal)			
			7.2ky	Early Bog Period (Atlantic)			
			9.3ky	Early Birch Period (Boreal)			
			10ky	Pre-Boreal			
		Upper Pleistocene	11Ky	Weichselian	Younger Dryas		Ice Age glacier disappears
			12ky		Allerød		Fossvogur sediments accumulate
			20ky		Older Dryas		
			70ky				Last glacial stage
			130ky	Eemian			Elliðavogur sediments accumulate Last interglacial
			170ky	Saale			Second last glacial stage
			700ky				Svínafell sediments accumulate
		Lower Pleistocene	2.5my			Plio-Pleistocene Formation	Rauðsgjá tillite Breiðavík tillite and sediments Furuvík tillite formed Full scale glaciation
	Tertiary	Pliocene	3.3my				Tjörnes sediments stop accumulating Pacific Ocean fauna arrives in Iceland Bearing strait opens
			7my			The Tertiary Basalt Formation	Tjörnes sediments begin to form First sign of cooling climate
		Upper Miocene	12my.				Warm temperate climate
		Middle Miocene	18my				Oldest rock on land.
		Early Miocene	25my				Birth of Iceland

This activity has received funding from the European Institute of Innovation and Technology (EIT), a body of the European Union, under the Horizon 2020, the EU Framework Programme for Research and Innovation

5.2. Description of volcanic systems in Iceland

A volcanic system is the principal geological structure in Iceland. It consists of a fissure swarm or a central volcano, or both, which are surface expressions of two different types of subsurface magma holding structures: the first a deep-seated magma reservoir, the second a shallower crustal magma chamber (Figure 5). Each volcanic system is characterized by conspicuous tectonic architecture and distinct magma chemistry and typically has a lifetime between 0.5 - 1.5 million years. The fissure swarms are narrow and elongated strips (5 to 20 km-wide and 50 to 100 km-long) of tensional cracks, normal faults and volcanic fissures (Figure 5). They are the surface expressions of elongated magma reservoirs, which are situated at the base of the crust (>20 km depth). These swarms are typically aligned subparallel to the axis of their host rift zone, illustrating that the fundamental force responsible for their formation is plate pull. Wide cracks indicative of pure crustal extension are usually the most conspicuous structures on the surface. Fault scarps and graben are also common and indicate vertical displacement and extension of crustal blocks. Young volcanic fissures typically appear as a row of small volcanic cones, whereas subglacial fissures occur as elongated „móberg‟ ridges.

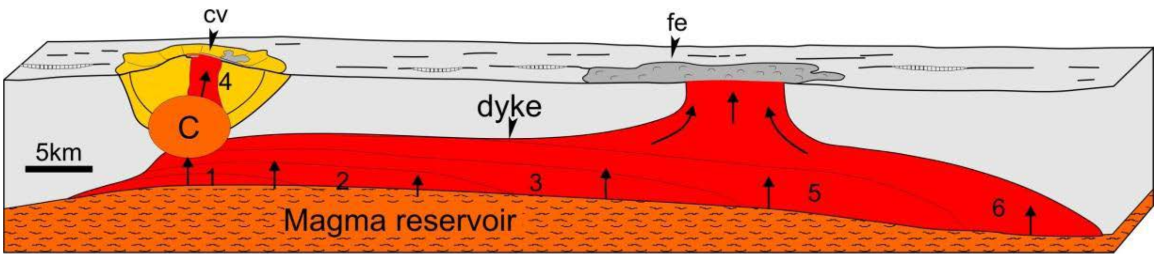

Figure 5. Upper figure: The main structural elements of a volcanic system. Abbreviations: c, crustal magma chamber; ds, dyke swarm; cv, central volcano; fs, fissure swarm; fe, fissure eruption. Lower figure: Injection and growth of a dyke feeding an eruption during a rifting episode. The numbers indicate the growth sequence of the dyke rising through the crust in a major eruption episode (taken from Thordarson, 2012).

5.3. Description of high -temperature geothermal systems in Iceland

Active systems

Most of the high-temperature areas in Iceland are located at the plate boundary where it is intersected by a fissure swarm. Volcanic activity is most intense at these points of intersection. In

This activity has received funding from the European Institute of Innovation and Technology (EIT), a body of the European Union, under the Horizon 2020, the EU Framework Programme for Research and Innovation

the eastern volcanic belt, central volcanic complexes that rise above the lava plateau have formed at these points of intersection. In some of them calderas have formed (Arnórsson et al., 2008).

Figure 6 provide a simplified sketch of a hydrothermal system in Iceland. Driving by a heat source, fluids, in most cases meteoric origin, infiltrate into the basaltic crust and get heated up, which results in a hydrothermal convection cell. Upwards migration and resulting hydrostatic pressure decrease result in boiling of the geothermal fluid once the fluid crosses the conditions of the boiling point curves. Surface manifestation, such as steaming vents or mud pools are results of the boiling process in the subsurface. Warm and/or hot spring are a result of the outflow at groundwater level.

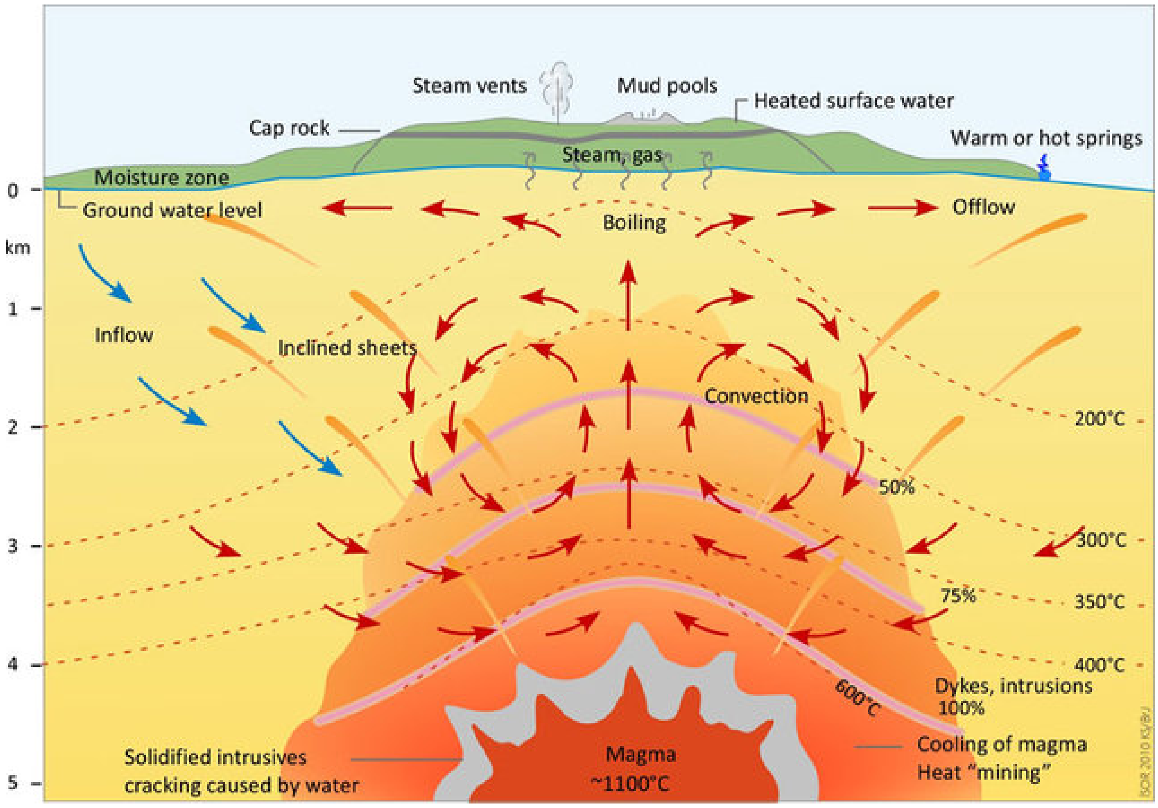

Figure 6. Simplified representation of hydrothermal systems in Iceland. The percentages indicate the fraction of intrusive material (dikes, sheets and minor intrusions) in the rock matrix (taken from Ketilsson et al., 2010).

Secondary alteration minerals form as a consequence of fluid-rock interaction at elevated temperatures and by the breakdown of the primary phases (Figure 7). Sequences of alteration minerals with increasing depth and temperature are identified as alteration zones in basaltic rocks in Iceland (e.g. Kristmannsdóttir, 1978; Weisenberger and Selbekk, 2009).

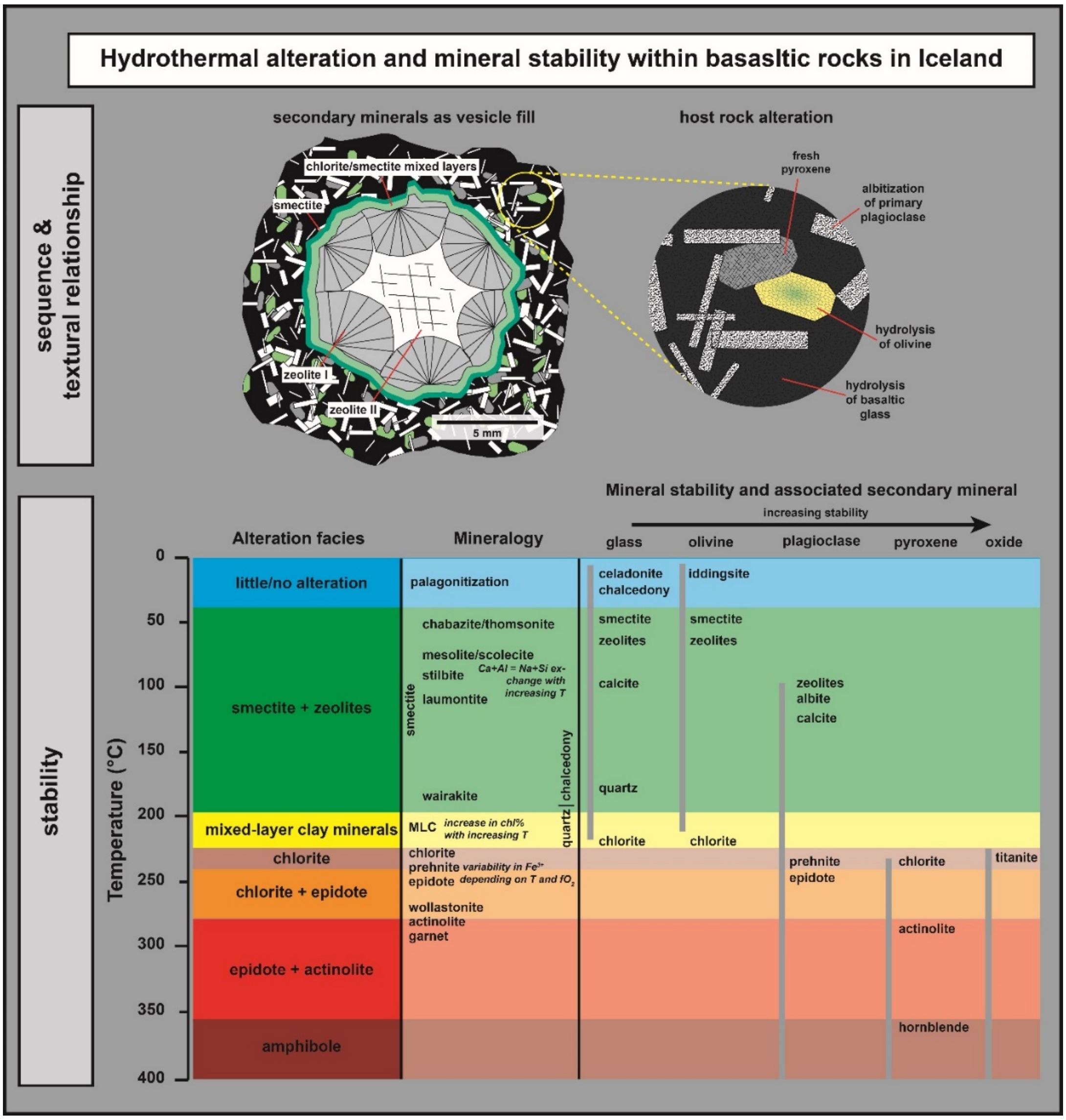

Figure 7. Stability fields of secondary minerals, including chemical vectors, primary minerals and their alteration product for basaltic rocks in Iceland. The sketch in the upper part shows a prograde mineral sequence as observed in Iceland geothermal system at low-temperature conditions (taken from Weisenberger at al., 2020 and modified after Kousehlar et al. 2012).

Fossil systems

Many fossil high-temperature geothermal systems in Tertiary and Lower-Quaternary formations have been exhumed by erosion (Figure 8). The volcanic complexes are typically embedded within

flood basalt sequences formed by fissure eruptions. These complexes are distinguished from the regional flood basalts by difference in dip and abundance of silicic and sometimes intermediate volcanic rocks. The silicic rocks are considered to have formed by partial melting of basaltic rocks overlying major magma reservoirs at the base of the crust.
The fossil high-temperature systems are represented by an aureole of alteration minerals enveloping and overlying a complex of minor intrusions within the central volcanic complex (Figure 7). Major gabbroic bodies, like those found in the most deeply eroded formations in the southeast part of the country, probably correspond to relatively high-level magma chambers that fed higher-level minor intrusions. These bodies in turn were likely fed by larger magma reservoirs at the base of the crust.

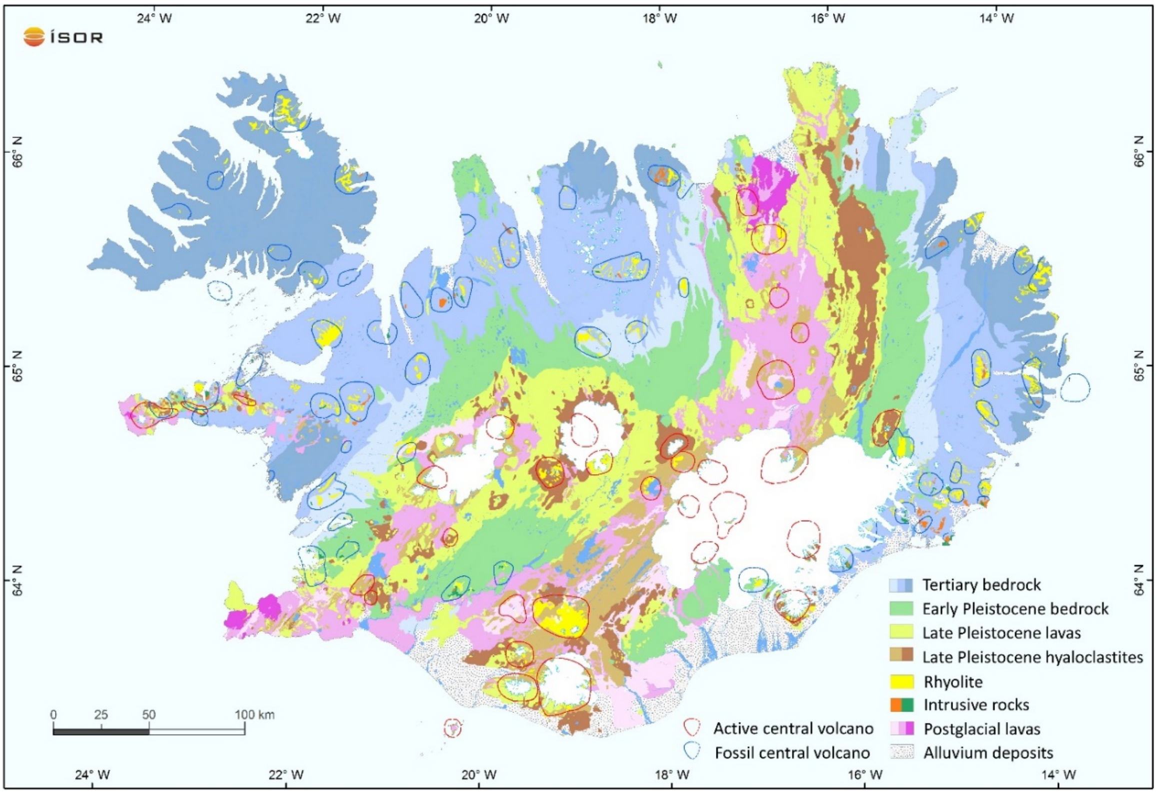

Figure 8. Geological map of Iceland showing Quaternary, including the volcanic zones, and Tertiary formations. Also shown are active central volcanoes and eroded, fossil central volcanoes (map taken from Franzson et al., 2016).

The altered lavas and intrusions of fossil high-temperature systems are characteristically green in color due to abundance of chlorite, and sometimes epidote. Other common hydrothermal minerals include calcite, quartz and sulphides, mainly pyrite, but many other hydrothermal minerals have been identified including actinolite, adularia, albite and garnet. This mineral

This activity has received funding from the European Institute of Innovation and Technology (EIT), a body of the European Union, under the Horizon 2020, the EU Framework Programme for Research and Innovation

assemblage belongs to the lower-greenschist facies and is indicative of temperatures in excess of 250 °C. The alteration is sometimes pervasive, but it is more common that the rock has been partially altered in which case intrusions may be quite fresh as well as the massive central part of lava flows whereas the amygdaloidal upper parts of the lavas, which have the highest porosity and permeability, are typically intensely altered (Neuhoff et al., 1999; Weisenberger and Selbekk, 2009). The depth of intrusion may be inferred from estimates of the original top of the lava pile.

5.4. Epithermal gold in Iceland

Information of gold exploration in Iceland that is presented here is based on the work presented in Franzson et al., (2013, 2016).

Gold exploration in Iceland

Exploration for gold dates back to early 20th century (Kristjánsson 1929, Fridleifsson et al. 1997, Franzson et al., 2013). Björn Kristjánsson, a politician and a bank manager, and Einar Benediktsson, a famous poet and entrepreneur were the early prospectors who found a number of gold rich locations (Franzson et al., 2013). The most notable are in Mogilsá north of Reykjavík and in Þormodsdalur (Figure 9). The latter, a multiple quartz vein was explored by tunneling and surface excavations. The exploration apparently stopped due to economic recession in Europe during and following the First World War (Franzson et al., 2013).

Renewed interest of gold exploration in Iceland developed about 1989 when the close connection between thermal activity and gold deposition, even in low salinity environments, became apparent. This led to limited reconnaissance surveys financed by private and governmental sources, later followed up by the exploration companies Malmis/Melmi and Sudurvik which made extensive, low-density reconnaissance surveys in eroded sections of the country (Franzson et al., 1992, Franzson and Fridleifsson, 1993, Oliver, 1993, Franzson et al., 1995, 1997, 2013, 2016).

This activity has received funding from the European Institute of Innovation and Technology (EIT), a body of the European Union, under the Horizon 2020, the EU Framework Programme for Research and Innovation

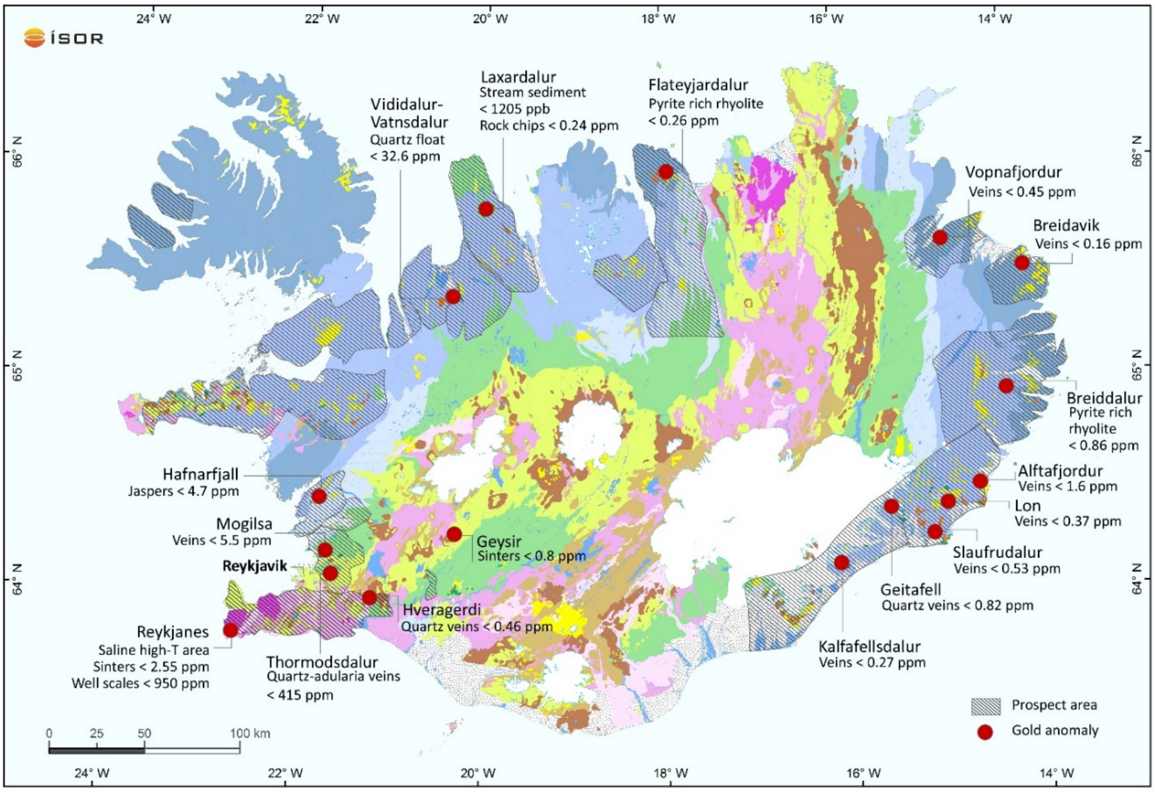

Figure 9. Map of gold anomalies discovered in Iceland as of 2015 and the prospect areas which have been explored to variable degree (taken from Franzson et al., 2016).

Exploration strategy

Good bedrock exposures with limited sedimentary and vegetation cover provides good conditions for exploration in Iceland. The target areas are fossil high-temperature systems within exhumed central volcanoes (Figure 8). The basic theme in the exploration has been the epithermal origin of gold which would imply targets limited to relatively shallow parts of the geothermal systems, i.e. above about 1000 m depth (Franzson et al. 1992, Franzson and Fridleifsson 1993). Geothermal systems in Iceland have been viewed as multiphase, extending up to 1 myr in age, with thermal conditions changing according to the appearance of heat sources and/or renewed pathways for the in-/outflow of geothermal fluids. Areas around larger intrusive bodies at the base of the central volcanic complexes are also of interest for exploration, mainly for possible evidence of metalliferous magmatic volatiles. It should though be taken into consideration that magmas from oceanic crustal environment are expected to have lower volatile contents than those derived from subduction or continental environments. Base metals in high concentrations have not been found in Iceland, except at two locations in the southeast, both associated with volatiles from a rhyolitic magma source (Jankovic, 1970, Franzson and Fridleifsson, 1993). The main exploration methods used are stream-sediment, rock and grab sampling. A summary of the exploration results is shown in Figure 9 (Franzson et al., 2016). During the course of the project available data has been included in an ArcGIS database (Figure 10 to Figure 13).

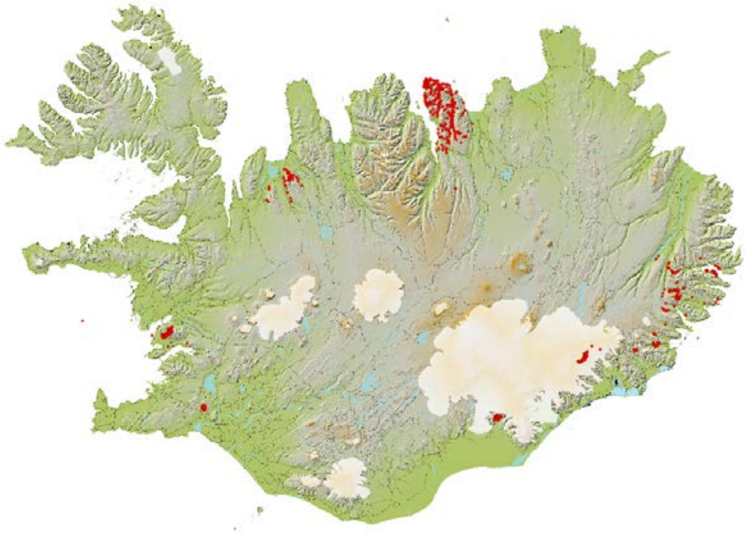

Figure 10. Data points for geochemistry data (rock chips).

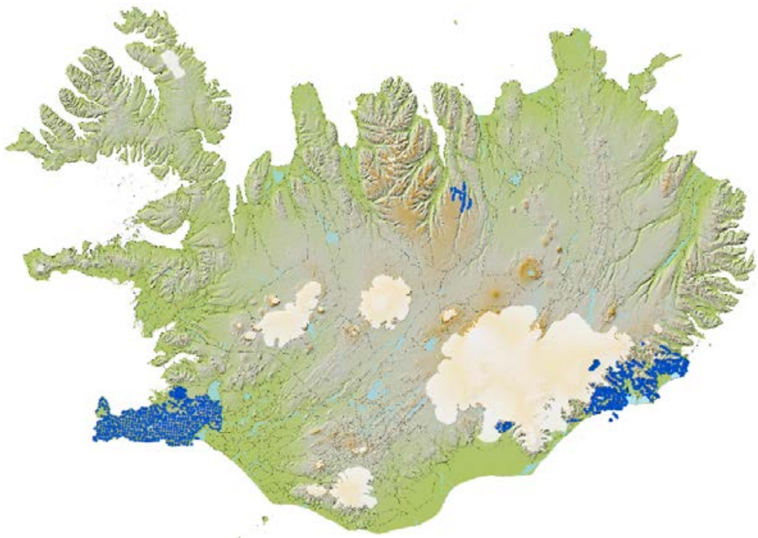

Figure 11. Data points for geochemistry data (soil samples).

This activity has received funding from the European Institute of Innovation and Technology (EIT), a body of the European Union, under the Horizon 2020, the EU Framework Programme for Research and Innovation

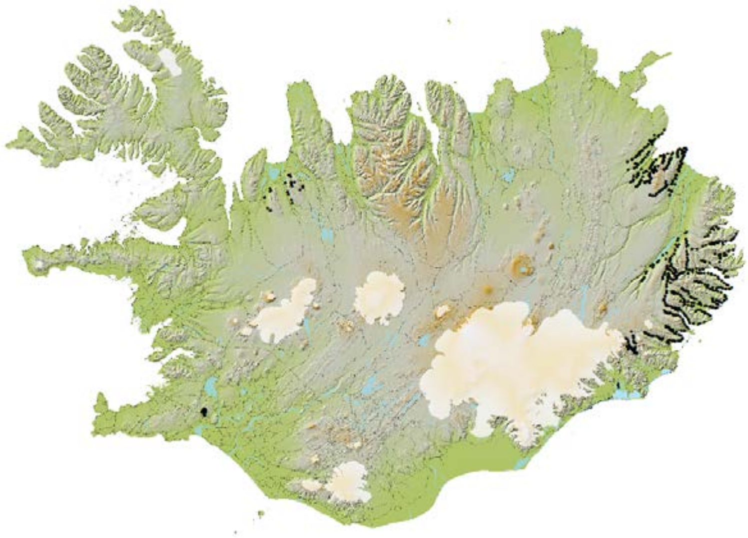

Figure 12. Data points for geochemistry data (stream samples).

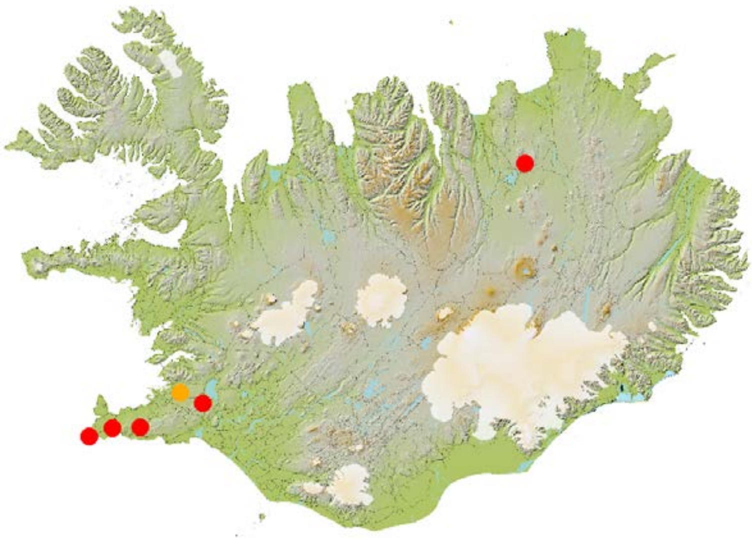

Figure 13. Data points for geochemistry data (borehole cuttings).

Prospects

As seen Figure 9 there are two prospect area outstanding (Mogilsá and Þormóðsdalur) which are described here in more detail based on the summary presented in Franzson et al. (2016).

This activity has received funding from the European Institute of Innovation and Technology (EIT), a body of the European Union, under the Horizon 2020, the EU Framework Programme for Research and Innovation

Mogilsá prospect: The Mogilsá prospect is located on the southern flanks of mount Esja about 20 km northeast of the capital Reykjavik (Figure 9). The interest in the area started in 1875 when mining of a thick calcite vein system for production of lime began. Later studies, around 1917, indicated the presence of gold in the veins, but efforts to establish a gold mine were aborted due to lack of belief in the analytical data (Franzson et al., 2016).

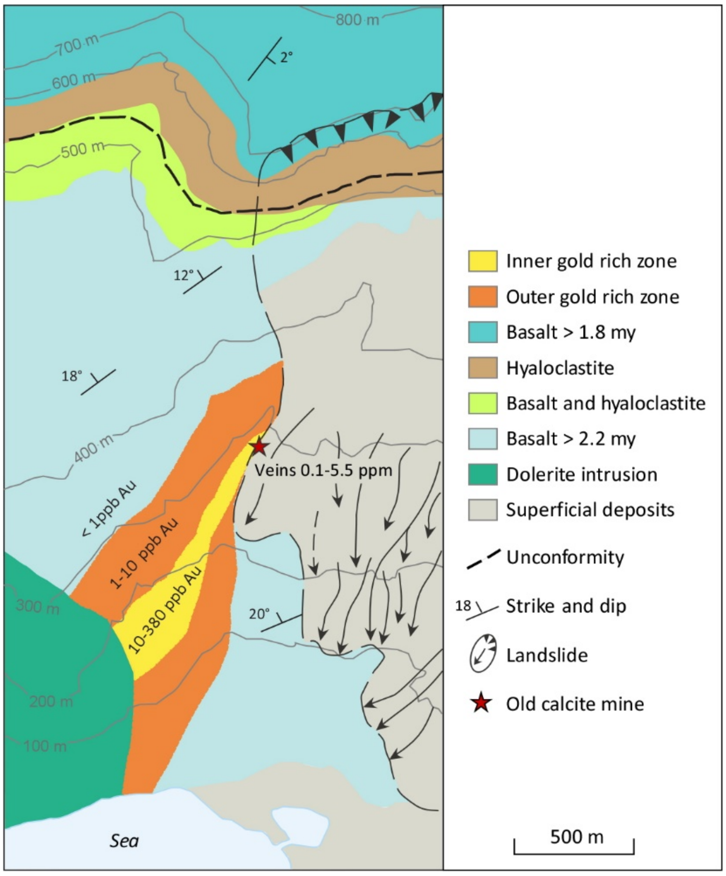

Figure 14. Map of the Mogilsá gold anomaly showing the BLEG gold values in the inner and outer zones (taken from Franzson et al., 2016).

Renewed gold exploration in the late 1980s confirmed the enrichment of gold in the area. The area shows high-temperature alteration with chlorite-epidote alteration around sea level and chlorite reaching up to 400 m elevation, mainly related to a NE-SW-trending, heavily sulphidized zone. This zone contains gold enrichment which was defined by profiles using BLEG (Bulk Leach Extractable Gold) analytical methods and shown in Figure 14. The anomaly is concealed towards the northeast, where it disappears under a recent landslide. The BLEG gold values in the outer zone range from 1 - 10 ppb and in the inner zone from 10 - 380 ppb. This is concomitant with

This activity has received funding from the European Institute of Innovation and Technology (EIT), a body of the European Union, under the Horizon 2020, the EU Framework Programme for Research and Innovation

increasing sulphidization, which is most intense in the inner zone, where sampling of veins shows gold contents from 0.1 to 5.5 ppm. Breccia in the core of the veining system suggests the presence of a hydrothermal explosion breccia. Hydrothermal alteration of the rocks indicates intense chloritization at the time of gold enrichment. A fluid inclusion study shows a Th-temperature range of 200 - 270 °C which conforms to a boiling-point curve depth of 300 - 500m. An unconformity occurs some 300 m above the main anomaly, seen both as a change in strata inclination and alteration. The unconformity probably represents the surface of the geothermal system at the time of ore formation, during a state of intense boiling, a very favorable condition for gold precipitation (Franzson et al., 2016).
Figure 15 shows the conceptual model of the geothermal system and the location of the anomaly deduced from the field study. It predicts the presence of a broader, underlying geothermal reservoir narrowing upwards along a tectonic lineament. The intense sulphide zone indicates the presence of an underlying, degassing magma intrusion. The Mogilsá area lies within a very popular mountain hiking route, which may lead to public reservations regarding permits for exploration drilling and exploitation (Franzson et al., 2016).

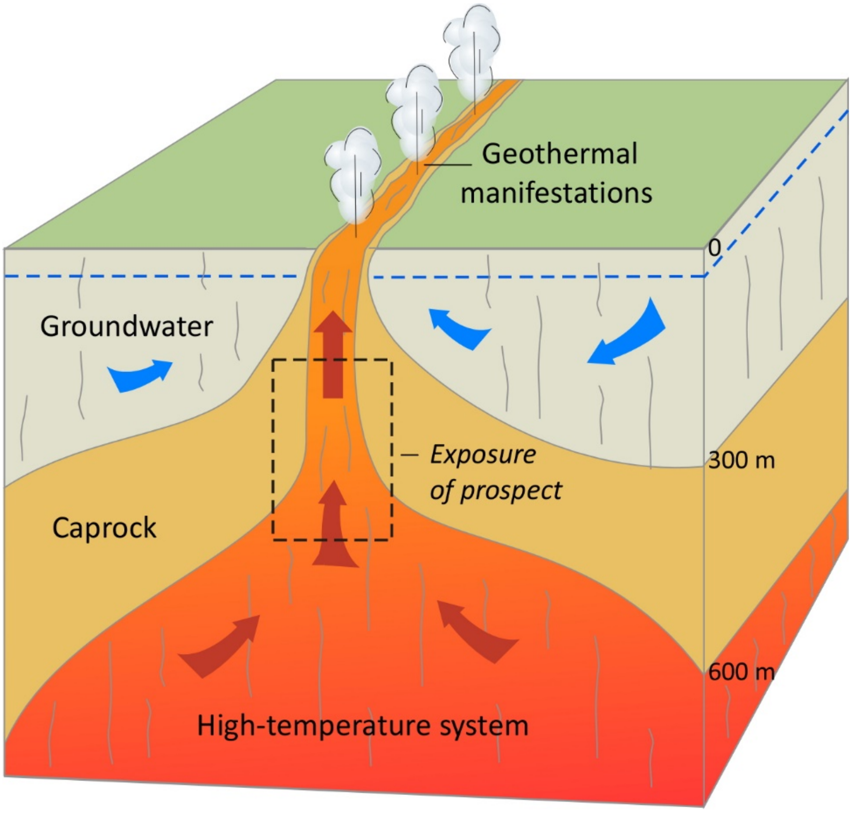

Figure 15. Conceptual model of the Mogilsá geothermal system (taken from Franzson et al. 2016).

This activity has received funding from the European Institute of Innovation and Technology (EIT), a body of the European Union, under the Horizon 2020, the EU Framework Programme for Research and Innovation

<u>Þormóðsdalur prospect:</u> The Þormóðsdalur prospect is anomalous in Iceland in relation to gold enrichment. It is located about 10 km east of the capital Reykjavik (Figure 9). Initial exploration of the locality was made by a local farmer and his family and then further aided by the poet and entrepreneur Einar Benediktsson: Over 300 m of excavations and tunneling were achieved during 1908 - 1925 by three consecutive exploration companies. The rocks were at one stage exported to Germany, but reports of their Au content remain speculative (Fridleifsson et al., 1997; Franzson et al., 2016).

The country rock is dominantly pillow-rich hyaloclastites with subordinate sub-aerial lavas. The strata dips about 12°SE. The area may belong to the Stardalur Central Volcano (1.5 - 2 myr) located about 6 km to the northeast (Fridleifsson, 1973), although it is closer to the Kjalarnes central volcano. The prospect area is within the chabazite-thomsonite alteration zone, indicating a low temperature environment (30 - 50 °C) and a burial depth of 300 - 500 m. However, data from nearby wells to the north show an underlying propylitic alteration due to a fossil high-temperature reservoir, belonging to the Stardalur Central Volcano (Franzson et al., 2016).

The area is densely faulted, mostly by NE-SW-trending faults parallel to the rift fractures. More northerly normal faults with a dextral strike-slip component and fracture trends are also evident. Their occurrence may be related to the structural change from a normal rift to the hybrid rift-transform environment of the Reykjanes Peninsula to the south. The Þormóðsdalur structure belongs to the latter northerly trend and has thus a transform character. This fault has been traced for about 700 m (Figure 16; Franzson et al., 2016).

Petrographic and XRD studies show the evolution of the vein system from a zeolite assemblage to quartz-adularia indicating progressive heating of the system and lastly to a minor calcite. The Au-enriched zone belongs to the quartz-adularia assemblage. A preliminary SEM study shows Au-grains up to 20 µm across. Temperature estimates based on mineral zonation and a limited fluid inclusion study suggest a range of 180 - 230 °C which concurs with a boiling condition of the geothermal system at approx. 300 m depth (Franzson and Fridleifsson 1993). A review of the data suggests that the deposit is categorized as a low-sulphidization, adularia-sericite, epithermal Au-Ag type (Corbett, 2004). The limited wall rock alteration suggests that this part of the geothermal system may have been relatively short-lived but intense (Franzson et al., 2016).

Forty-one cored wells have been drilled into the vein system, totaling nearly 3000 m. These wells generally extend to <100 m, many of them inclined. They indicate significant grades and thicknesses confined to two shoots along the vein structure (Fleming et al., 2006). A 450 m deep, temperature-gradient well was, in addition, drilled slightly to the west of the vein system, where it is intersected Au-enriched veins at depths down to 450 m. The Au grades of the veins in the wells are variable, which is not surprising considering the mineral evolution discussed above: they range from <0.5 ppm to a maximum of 415 ppm (40 cm core sample in one well) (Franzson et al., 2016).

This activity has received funding from the European Institute of Innovation and Technology (EIT), a body of the European Union, under the Horizon 2020, the EU Framework Programme for Research and Innovation

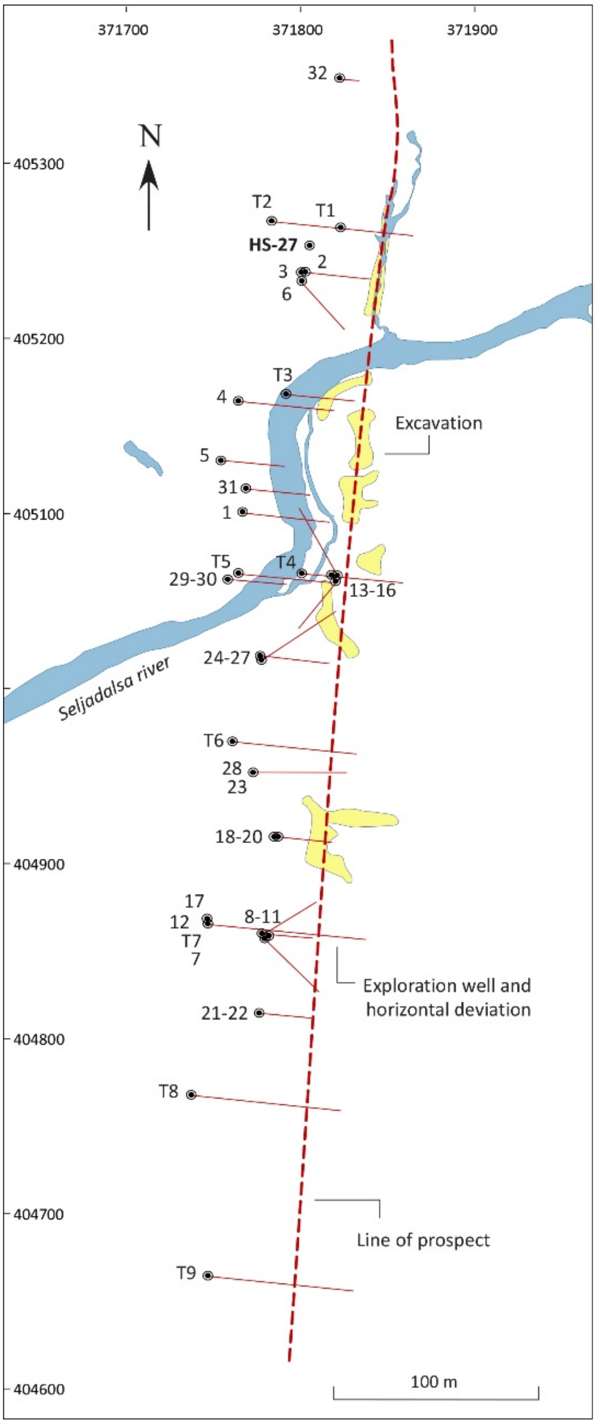

Figure 16. Map showing the alignment of the quartz-adularia vein and the location and horizontal projection of the 41 drillholes at Þormóðsdalur (taken from Franzson et al., 2016).

This activity has received funding from the European Institute of Innovation and Technology (EIT), a body of the European Union, under the Horizon 2020, the EU Framework Programme for Research and Innovation

Ore formation model

The formation of epithermal deposits is a complex system. Require information to establish full ore formation model include information on the metal source, fluid origin, migration pathways for fluids, ore traps as well as the energy that drive the hydrothermal system (Figure 17).

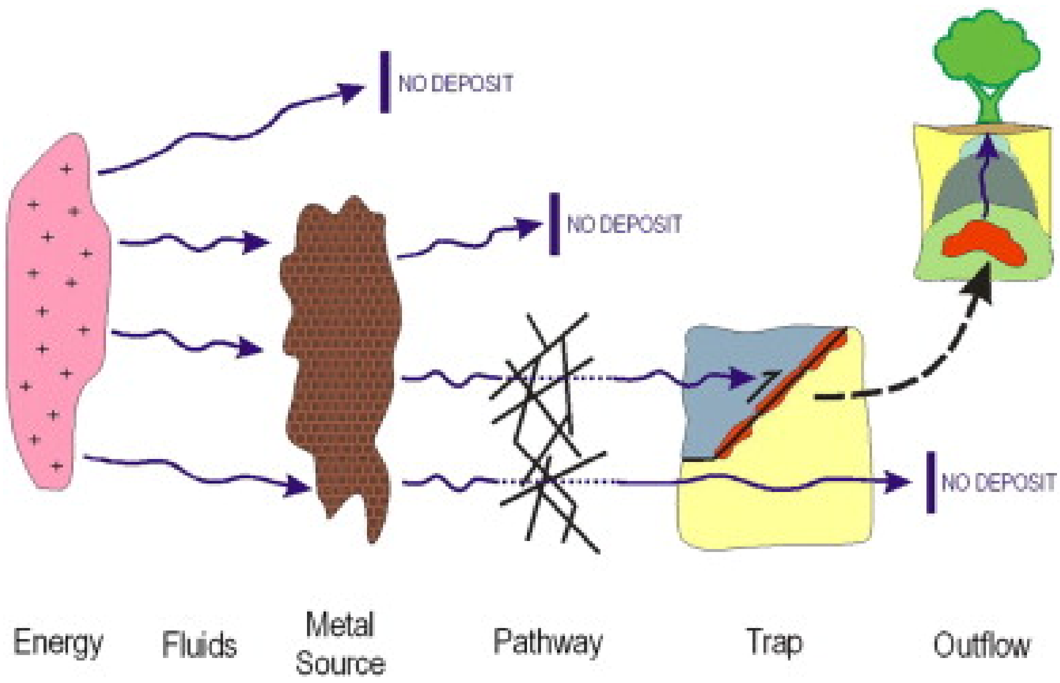

Figure 17. The mineral systems concept of ore formation from source of energy and metal through transport to trap (taken from Payne et al., 2015).

Mineral exploration is still in its infant stages in Iceland and therefore only very limited information are available. The hydrothermal systems associated with ore formation process are associate with central volcanoes. In Iceland central volcanoes can be classified as active and fossil (Figure 8). Studies within active volcanic system (e.g. Hardardottir, et al., 2009; Hannington et al., 2016; Grant et al., 2020) shows the gold mobilization. Nevertheless, the active systems are not suitable for mining due to the high temperature as well as depth level. Shallow seated magma bodies provide the heat source for the hydrothermal central volcanic system. But it remains unclear what are the source rock for gold and other precious elements. Studies form recent and fossil hydrothermal system indicate meteoric water as major fluid source that get infiltrated into the crust and form the fluid convention cell once heated up by the heat source. Fluid geochemistry plays an important role when considering metalliferous epithermal environment. Sulphur is common in the high-temperature systems and is considered to be the main carrier of

This activity has received funding from the European Institute of Innovation and Technology (EIT), a body of the European Union, under the Horizon 2020, the EU Framework Programme for Research and Innovation

metals. In general, salinity is important transport agent of metalliferous complexes This is not the case in the Icelandic environment where meteoric water dominates in the geothermal systems with chlorine content less than 200 ppm (Franzson et al., 2016). It is assumed that fracture act as dominate fluid pathways and once boiling occurs precipitation occurs. This indicates that the deposits are formed relatively shallow within the maximum 1 to 1.5 km depth However, it still remains unclear what are prefer traps for gold precipitation within the central volcano.
Franzson et al. (2020) reported that primary gold concentrations in Icelandic volcanic formations range from 0.5 to about 20 ppb with an average value of 3.6 ppb (Zentilli et al., 1985; Nesbitt et al., 1986; Geirsson 1993). These are higher values than the 2 ppb quoted for regular mid-oceanic ridge basalt (MORB) (Peach et al., 1990).

6. Assessment of epithermal gold in Iceland

In following two chapters, the assessment of epithermal gold in Iceland is presented as part of the testing workshop.

On September 16th and 17th, 2020 a testing workshop was organized at the main office of the Iceland GeoSurvey (ÍSOR) in Reykjavík, Iceland. Due to restriction regarding the Covid-19 situation only experts from Iceland where physical present during the workshop. In order to allow other MAP consortium members to participate the online the platform Microsoft Teams.
Figure 18 shows the agenda of the workshop. Following expert from Iceland participated in the workshop: Hjalti Franzson (ÍSOR), Guðmundur Ómar Friðleifsson (IDDP), Vigdís Harðardóttir (GRO-GTP), Bryndís Guðrún Róbertsdóttir (Orkustofnun), Gunnlaugur M Einarsson (ÍSOR), and Tobias Björn Weisenberger (ÍSOR).

This activity has received funding from the European Institute of Innovation and Technology (EIT), a body of the European Union, under the Horizon 2020, the EU Framework Programme for Research and Innovation

Mineral Resource Assessment Platform (MAP)

Testing Workshop: Epithermal Gold in Iceland

September 16 & 17, 2020

September 16: 2020, 9:00-12:00

9:00-9:20: Introduction (*Tobias Björn Weisenberger*)

9:20-9:50: Epithermal Gold in Iceland (*Hjalti Franzson*)

Break

10:15-10:30: Exploration of Geothermal Gold in Iceland (*Guðmundur Ómar Friðleifsson*)

10:30-10:45: Gold within hydrothermal fluids (*Vigdís Harðardóttir*)

10:45-11:30: Discussion on epithermal gold potential in Iceland (G/T model, permissive tracts, ore forming process & conditions) (*Tobias Björn Weisenberger*)

11:30-12:00: Estimating undiscovered epithermal gold deposits in Iceland (*Tobias Björn Weisenberger*)

September 17: 2020, 9:00-12:00

9:00-9:30: Summary of first day (Tobias Björn Weisenberger)

9:30-10:45: MAP software Epithermal Gold in Iceland (Gunnlaugur M Einarsson)

Break

11:00-12:00 Discussion (Tobias Björn Weisenberger)

Figure 18. Agenda of the testing workshop in September 2020.

6.1. Descriptive model

Following the descriptive model for epithermal gold formation is described.

Model name:

Epidermal gold in Iceland

This activity has received funding from the European Institute of Innovation and Technology (EIT), a body of the European Union, under the Horizon 2020, the EU Framework Programme for Research and Innovation

Summary description:

In general, low-sulphidization epithermal deposits form in the upper crust at the paleosurface to depths about 1,500 m below the water table and at temperatures that range from about 100 to 300 °C. Although, low-sulphidization epithermal system may be dominant, medium- and high-sulphidization system cannot be excluded. Deposits are genetically related to hydrothermal systems associated with subaerial volcanism and intrusion that are related to central volcanic systems.

General references:

General references are: Franzson et al. (2016), John et al. (2018), Taylor et al. (2007), and White and Hedenquist (1995).

Deposits examples:

There are no gold deposits in Iceland. However, there are two promising prospect areas that include Mogilsá and Þormóðsdalur (Franzson et al., 2016).
Although there are many epithermal gold deposits know worldwide, no other deposits that exists at similar geological setting is known. An overview of existing epithermal gold (-silver) deposits is provided in John et al. (2018).

Geological environment:

The host rocks for deposits are central volcanos that are characterized by bimodal chemistry (basaltic and rhyolitic). Felsic volcanic centers and their associated structural zones. Gold is not inferred to be directly hosted by silicic rocks but is re-distributed by hydrothermal process which are often focus of these zones. Gold weakly tracks the trend of incompatible elements and may be shown to be re-mobilized from differentiated volcanic rocks during hydrothermal alteration (Zentilli et al. 1985). Fluids are dominantly meteoric fluids, with low salinities.

Age:

Plio-Pleistocene and Tertiary. Only fossil hydrothermal systems are considered.

Mineralization environment:

Hydrothermal systems associated with central volcanoes.

This activity has received funding from the European Institute of Innovation and Technology (EIT), a body of the European Union, under the Horizon 2020, the EU Framework Programme for Research and Innovation

Tectonic setting:

Oceanic rift & mantle plume

Mineralogy:

Although the alteration within hydrothermal systems of central volcanoes are well constrained (Figure 7), it remains unclear is the characteristic mineralogy of gold deposits. Based on the information know form the prospect areas the major gangue mineral associate with epithermal gold are quartz and calcite, as well as pyrite as major sulfide.

Texture and structure:

It is assumed that deposits are structural controlled. Due to the lack of existing deposits, it remains unclear what are deposit controlling structure, as well as the extend.

Ore control:

Structural controlled within hydrothermal systems of central volcanoes.

Alteration:

Classic alteration style within basaltic hydrothermal systems from low to high alteration: unaltered, smectite-zeolite, mixed-layer clays, chlorite, epidote, actinolite. However, a well

Geochemical signature:

Gold in Icelandic rocks loosely tracks the trend of incompatible elements, such as Y and Zr.

This activity has received funding from the European Institute of Innovation and Technology (EIT), a body of the European Union, under the Horizon 2020, the EU Framework Programme for Research and Innovation

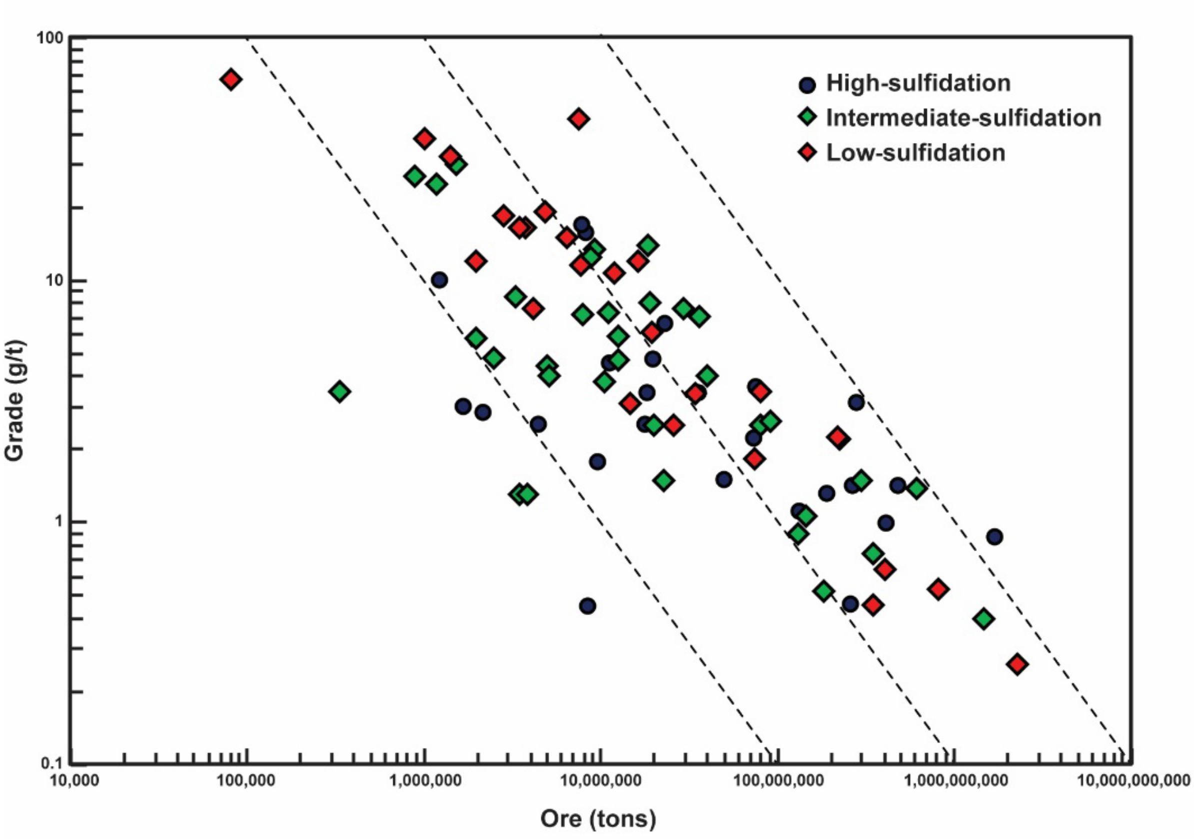

Figure 19. Graphs showing gold grades and tonnages for most epithermal gold/silver deposits summarized in John et al., (2018). Ore tonnages are a combination of production, proven and probable reserves, and measured and indicated resources, where available. Grades are averages of all ore types. Diagonal lines show total contained metal in metric tons.

6.2. Grade/tonnage model

The grade/tonnage model (Figure 19) used for the assessment is taken from the recent USGS compilation by John et al. (2018). Epithermal gold deposits range in size from tens of thousands to greater than 1 billion metric tons of ore and have gold contents of 0.1 to greater than 30 grams per metric ton (g/t).

This descriptive model of epithermal gold(-silver) deposits is part of a systematic effort by the U.S. Geological Survey Mineral Resources Program to update existing, and develop new, descriptive mineral deposit models. The U.S. Geological Survey deposit modeling effort is intended to

This activity has received funding from the European Institute of Innovation and Technology (EIT), a body of the European Union, under the Horizon 2020, the EU Framework Programme for Research and Innovation

supplement these summaries by developing more complete models in a common format for use in mineral-resource and mineral-environmental assessments (John et al., 2018).
The grad/tonnage model show a relatively large range (Figure 19). The compilation by John et al. (2018) includes deposit throughout the globe from various geological setting. However, not any single deposits in similar geological setting than Iceland is known and can be used for direct comparison. Therefore, it needs to be pointed out the grade/tonnage model should be considered critical.

6.3. Permissive tract

Permissive tracts were delineated epithermal gold deposits in Iceland based on the ore formation model as well as the minable accessibility. In a first discrimination the neo-volcanic zone of Iceland has been excluded (Figure 20) and only the Tertiary and Plio-Pleistocene units are considered. On one hand this are area is volcanic active and it is assumed that within the active zone, deposit formation is still ongoing. Further this area is characterized by active hydrothermal system and the higher geothermal gradient will not allow any mining
In a next step fossil volcanic system are delineated within the Tertiary and Plio-Pleistocene units. The fossil volcanic centers are central volcanoes that are characterized by hydrothermal system, that show an alteration aureole, as well as bimodal volcanism. The fossil central volcanoes are based on the geological map by Hjartason and Sæmundsson (2014) and are delineated in Figure 21.
For this assessment three representative central volcanoes are selected (Figure 21). This include the Breiðdalur central volcano in East Iceland that has been intensively studied by Walker in the 1960 (e.g. Walker, 1960, 1963; Askew, 2020) the Hafnarfjall central volcano in west Iceland which has been extensively studies by Franzson (1978) and the Kjarlanes/Stardalur central volcano in southwest Iceland that host the two prospect areas Mogilsá and Þormóðsdalur (Franzson et al., 2013, 2016).

This activity has received funding from the European Institute of Innovation and Technology (EIT), a body of the European Union, under the Horizon 2020, the EU Framework Programme for Research and Innovation

Figure 20. Outline of Iceland. The gray area marks “older” volcanic rock (Tertiary and Plio-Pleistocene) based on the geological map by Hjartarson and Sæmundsson (2014). The neo-volcanic zone (white area) has been excluded.

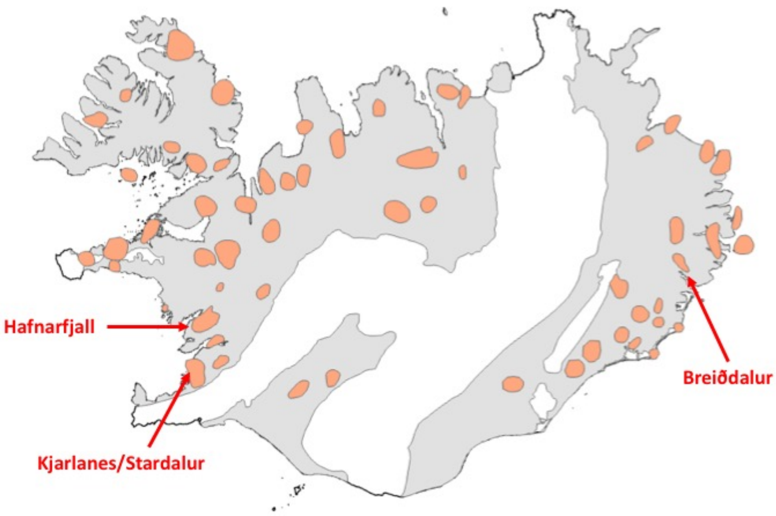

Figure 21. Outline of Iceland. The gray area marks “older” volcanic rock (Tertiary and Plio-Pleistocene). The orange delineated area are fossil central volcanoes which are based on the geological map by Hjartarson and Sæmundsson (2014). The three selected central volcanoes that are assessed are marked.

This activity has received funding from the European Institute of Innovation and Technology (EIT), a body of the European Union, under the Horizon 2020, the EU Framework Programme for Research and Innovation

Breiðdalur

Breiðdalur is situated west of the town of Breiðdalsvík, and the first exposures of Breiðdalur volcanics, part of the Breiðdalur volcanic system, are found around 18 km along route 1 from the town (Figure 22). Due to the roughly east–west trend of valleys and fjords through westward dipping stratigraphy, the same units may be found in valleys and fjords to the north or south. The lowermost central volcano units, found in Berufjörður to the south, are located close to the farm of Gautavík, around 35 km from the town of Djúpivogur or 30 km from Breiðdalsvík. Many of the units in this area are found up valley from the lower exposure. The caldera is exposed at the head of Breiðdalur valley and a small sliver along Selá, Berufjörður. Silicic volcanic rocks are located across the peaks of northern Berufjörður and above Þorgrímsstaðir in Breiðdalur.

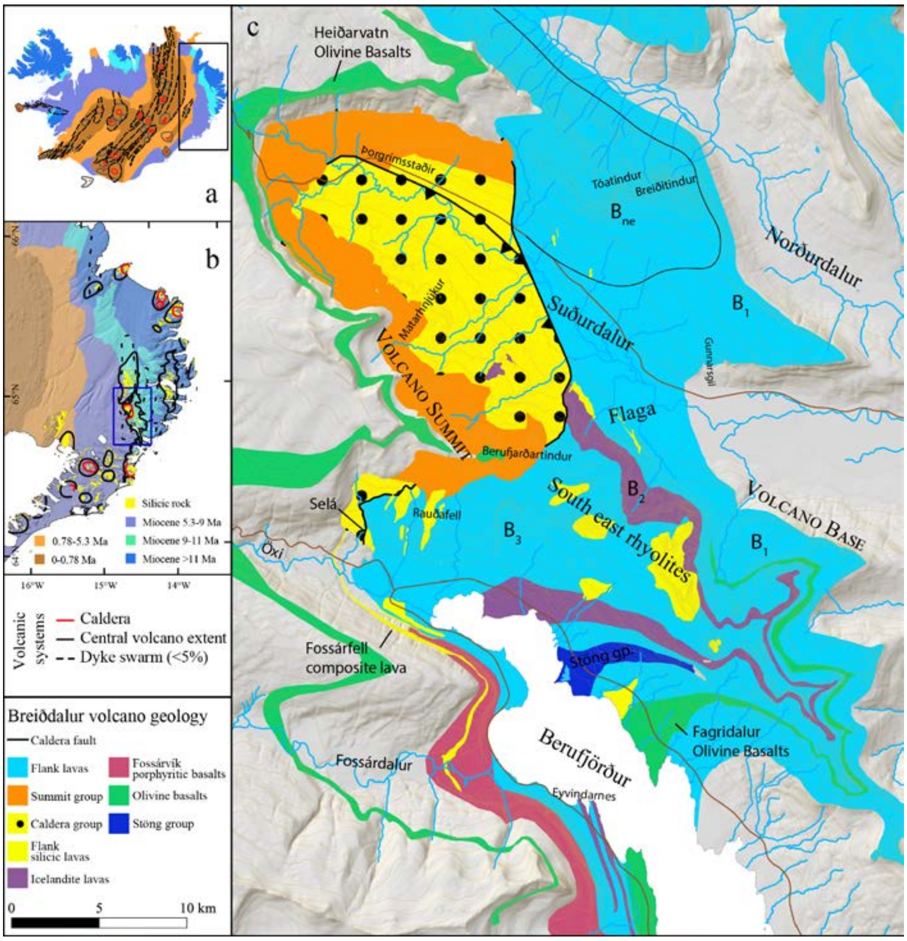

Figure 22. Geology of the Breiðdalur. a) Icelandic geology, black box is: b) east fjords volcanic systems, Breiðdalur shown in in the blue box. c) Breiðdalur volcano geology and localities, B1: Lower eastern flank sequence, B2: Icelandite lava sequence, B3: Upper eastern flank sequence and Bne: North eastern flank sequence. Samples were taken from within the volcano and the plateau basalt envelope around the volcano) (taken from Askew, 2020).

This activity has received funding from the European Institute of Innovation and Technology (EIT), a body of the European Union, under the Horizon 2020, the EU Framework Programme for Research and Innovation

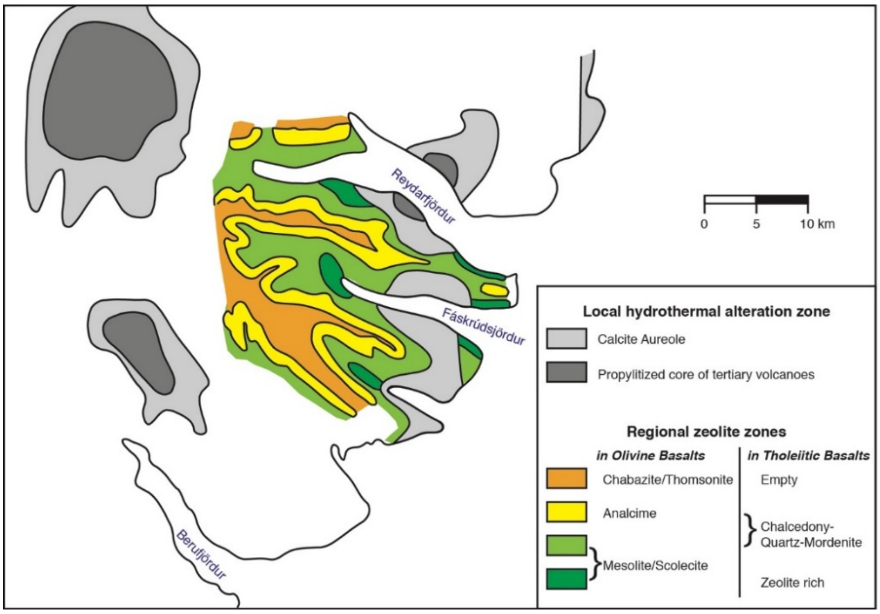

Figure 23. *Map showing distribution of regional zeolite zones, local hydrothermal zones and distribution of Tertiary volcanic centers (after Mehegan et al., 1982). The Breiðdalur central volcano is the lower left most aureole within the map.*

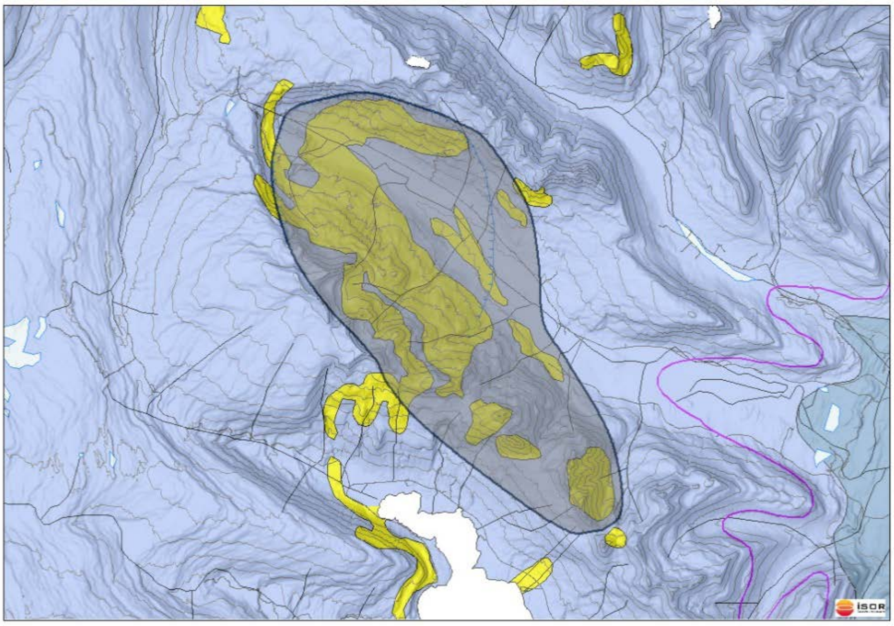

Figure 24. Extend of the Breiðdalur central volcano (dark blue line,) overline on the geological map (based on Hjartarson and Sæmundsson, 2014).

This activity has received funding from the European Institute of Innovation and Technology (EIT), a body of the European Union, under the Horizon 2020, the EU Framework Programme for Research and Innovation

The Breiðdalur volcano was extensively mapped by George Walker in the 1950s and 60's (e.g. Walker, 1963). The work by Georg Walker also provided a conceptual model of a central volcano. Robert Askew revisited the area recently verified some details (Askew, 2020).
Various age dating method (see Askew, 2020 for details) indicate that the magmatic series was emplaced about 10 - 9 Ma. In the south east, estimations from zeolite alteration (Walker, 1960) and magma emplacement depth suggest around 2 km of material was removed through erosion, in the northeast approximately 1 km was removed (Gústafsson, 1992).
The Breiðdalur central volcano shows well developed alteration aureole as shown in Figure 23. Figure 24 shows the extend of the permissive tract of Breiðdalur central volcano.
Geochemical sampling (soil and rock chips) is only very sparse and does not indicate any gold anomaly. The data is not shown here due to confidentiality.

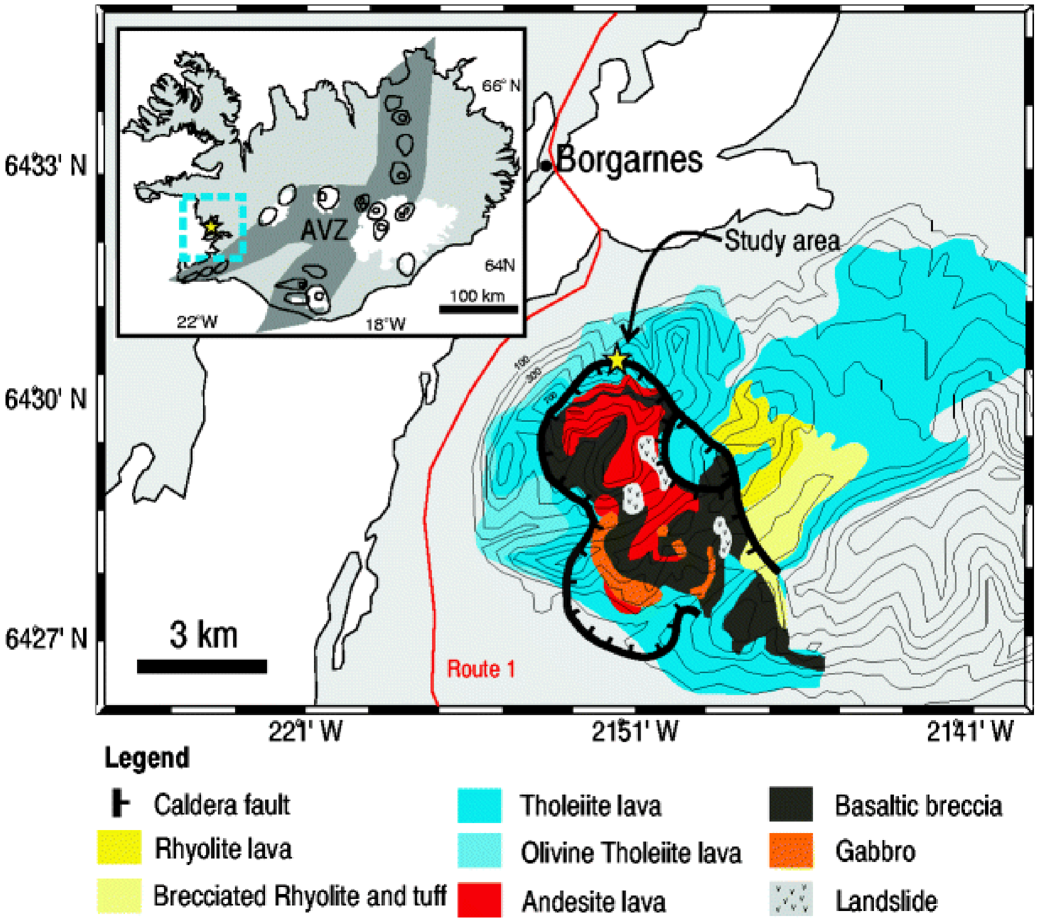

Figure 25. Geological map of Hafnarfjall central volcano, located in western Iceland, approximately 50 km northwest of the active volcanic zone (AVZ). The ring fault of the 7.5×5-km NW-SE elongated caldera is shown. Study area is marked with a yellow star. Taken from Browning and Gudmundsson (2015).

This activity has received funding from the European Institute of Innovation and Technology (EIT), a body of the European Union, under the Horizon 2020, the EU Framework Programme for Research and Innovation

Hafnarfjall

Hafnarfjall is an inactive and deeply eroded 5 Ma old central volcano (stratovolcano with a caldera) in western Iceland. The volcano is composed of a predominantly basaltic lava pile overlain by brecciated andesite and andesitic lava, as described in detail by Franzson (1978) (Figure 25). The volcano originally formed in the southwest volcanic zone of Iceland but subsequently drifted, through crustal spreading, 40 – 50 km (Gautneb et al., 1989) to the west-northwest of the rift zone. Hafnarfjall therefore offers the opportunity to study a caldera formed in a divergent plate boundary setting. Browning and Gudmundsson (2015) estimate that glacial erosion has removed the uppermost parts of the volcano based on the assumptions of Walker (1960) who used zonation of amygdale minerals to estimate the level of erosion in a nearby area. Hafnarfjall volcano contains numerous inclined sheets, predominantly basaltic, which dip on average at around 65°, trend NE, and have thicknesses that are commonly about 1 m or less (Gautneb et al., 1989).

Figure 26 shows the extend of the permissive tract of Hafnarfjall central volcano. Geochemical sampling (soil and rock chips) has been carried out in the SE part of the permissive tract. Although sampling is higher than the Breiðdalur permissive tract and gold values are slightly higher the data does not indicate any gold anomaly. The data is not shown here due to confidentiality.

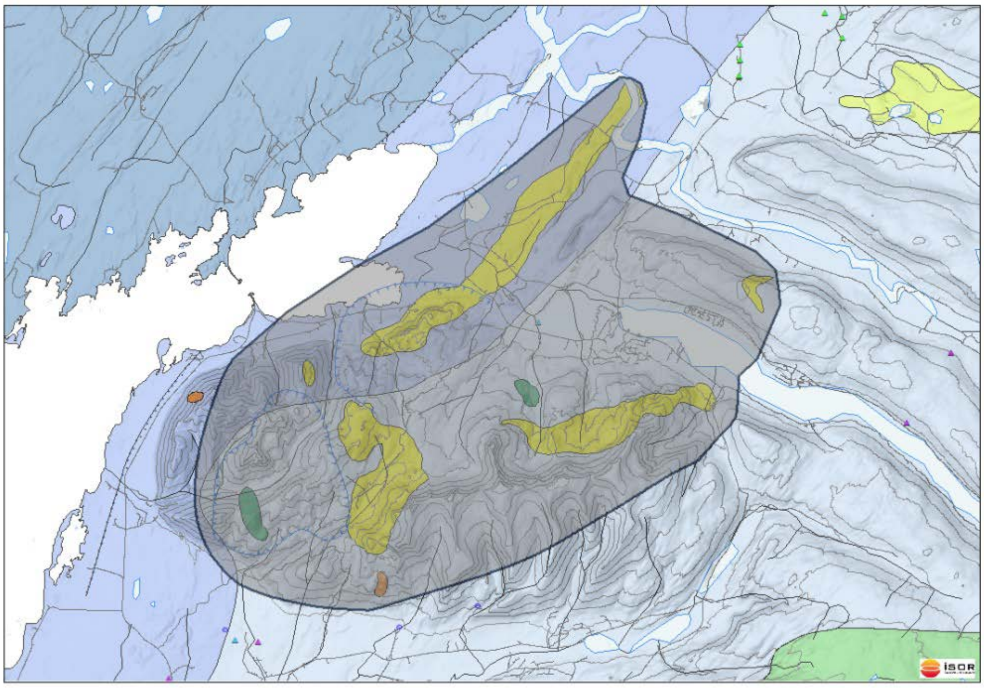

Figure 26. Extend of the Hafnarfjall central volcano (dark blue line) overline on the geological map (based on Hjartarson and Sæmundsson, 2014).

This activity has received funding from the European Institute of Innovation and Technology (EIT), a body of the European Union, under the Horizon 2020, the EU Framework Programme for Research and Innovation

Kjarlanes/Stardalur

Volcanism was active in the Esja region for just over one million years and during this time span, at least ten glaciations occurred in the region (Fridleifsson, 1973). The stratigraphy succession is therefore, characterized by a sequence of lava flows intersected with thick subglacial hyaloclastite units. Two central volcanos were active in the Esja region; the Kjalarnes volcano for about 0.6 million years which was succeeded after a short interval by the Stardalur volcano, which remained active for about 0.3 million years. Flood basalt volcanism was concomitant with the central volcanism and most of the olivine tholeiites are considered to have been erupted in fissures and shield volcanoes unrelated to the central volcanoes (Fridleifsson, 1973).
This permissive tract includes the well know prospect area of Mogilsá and Þormóðsdalur. Figure 27 shows the extend of the permissive tract of Kjarlanes central volcano. Geochemical sampling has been carried out at the prospect in Mogilsá and Þormóðsdalur. The data is not shown here due to confidentiality.

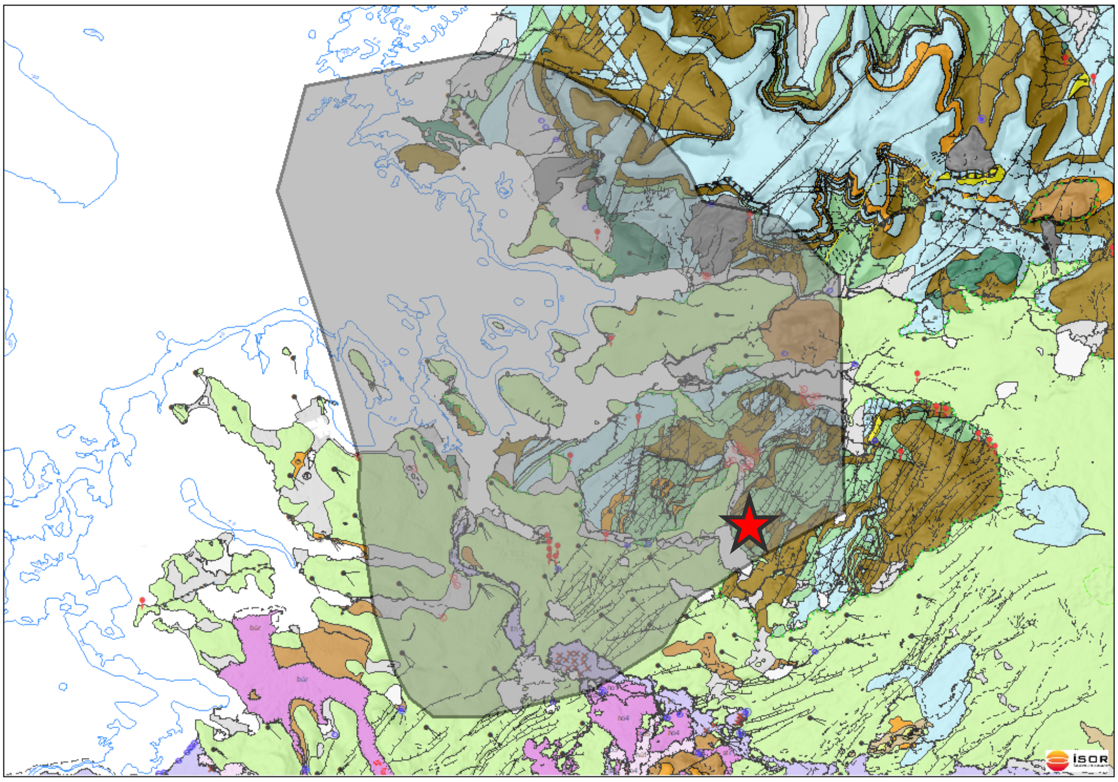

Figure 27. Extend of the Kjarlanes central volcano (dark blue line,) overline on the geological map (based on Hjartarson and Sæmundsson, 2014). The prospect Þormóðsdalur is marked by a red star.

This activity has received funding from the European Institute of Innovation and Technology (EIT), a body of the European Union, under the Horizon 2020, the EU Framework Programme for Research and Innovation

7. MAPWizard results

For testing we used MAPWizard 1.0.8.

7.1. Grade/tonnage model

The grade-tonnage model tool estimates probability density functions (Pdf) for ore tonnage and metal grade data or metal tonnage data of well-known deposits. The tool provides summary statistics and plots of the data and estimated probability distributions and saves the distribution probability density function for use in Monte Carlo simulation. The tool is based on and uses the R functions of the USGS software MapMark4 (Ellefsen, 2017a,b; Shapiro, 2018).
In total 85 deposits including low-, medium- and high-sulphidization type deposits based the compilation in John et al. (2018) have been used. The tool outputs the summary results and plots of the estimation and stores these results as well as the estimated probability density functions as R objects. Figure 28 the estimated metal grade probability density functions and data for 85 epithermal gold (-silver) deposits derived from the compilation in John et al. (2018). Table 3 shows the statistics for the gold grade data and the estimated probability density functions. Figure 29 shows the estimated ore tonnage pdf and data for epithermal gold (-silver) deposits used in the grade tonnage model. The deviance within the estimated ore tonnage is -22.5894. Table 4 and Table 5 provide a summary statistic for the ore tonnage or metal tonnage data and the estimated probability density function.

Table 3. Statistics for the metal (gold) grade data and the estimated probability density functions. Gatm refers to the actual grades from the grade and model; column probability density function (Pdf) refers to the pdf representing the grades.

Au	Gatm	Pdf
Minimum	0.0000026	0.0000001
0.25 quantile	0.0000150	0.0000169
Median	0.0000350	0.0000387
0.75 quantile	0.0001000	0.0000889
Maximum	0.0006790	0.0163000

This activity has received funding from the European Institute of Innovation and Technology (EIT), a body of the European Union, under the Horizon 2020, the EU Framework Programme for Research and Innovation

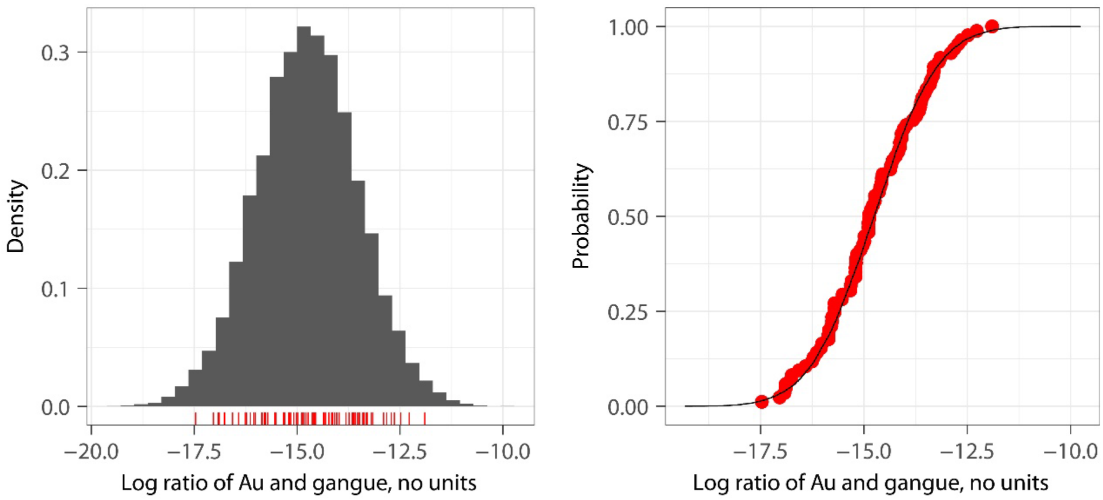

Figure 28. Plot of the estimated metal grade probability density functions and data for 85 epithermal gold (-silver) deposits derived from the compilation in John et al. (2018).

Table 4. Table pertains to the log-transformed tonnages. Gatm refers to the actual tonnages in the grade and tonnage model; column Pdf refers to the pdf representing the tonnages.

Au	Gatm	Pdf
Minimum	11.3	6.68
0.25 quantile	15.4	15.5
Median	16.7	16.9
0.75 quantile	18.3	18.3
Maximum	21.5	26.6
Mean	16.9	16.9
Standard deviation	2.09	2.09

Table 5. Table pertains to the (untransformed) tonnages. Gatm refers to the tonnages in the grade and tonnage model; column Pdf refers to the pdf representing the tonnages.

Au	Gatm	Pdf
Minimum	81000	795
0.25 quantile	4780000	5160000
Median	17800000	21100000
0.75 quantile	92100000	86200000
Maximum	2270000000	345000000000
Mean	145000000	185000000
Standard deviation	360000000	1410000000

This activity has received funding from the European Institute of Innovation and Technology (EIT), a body of the European Union, under the Horizon 2020, the EU Framework Programme for Research and Innovation

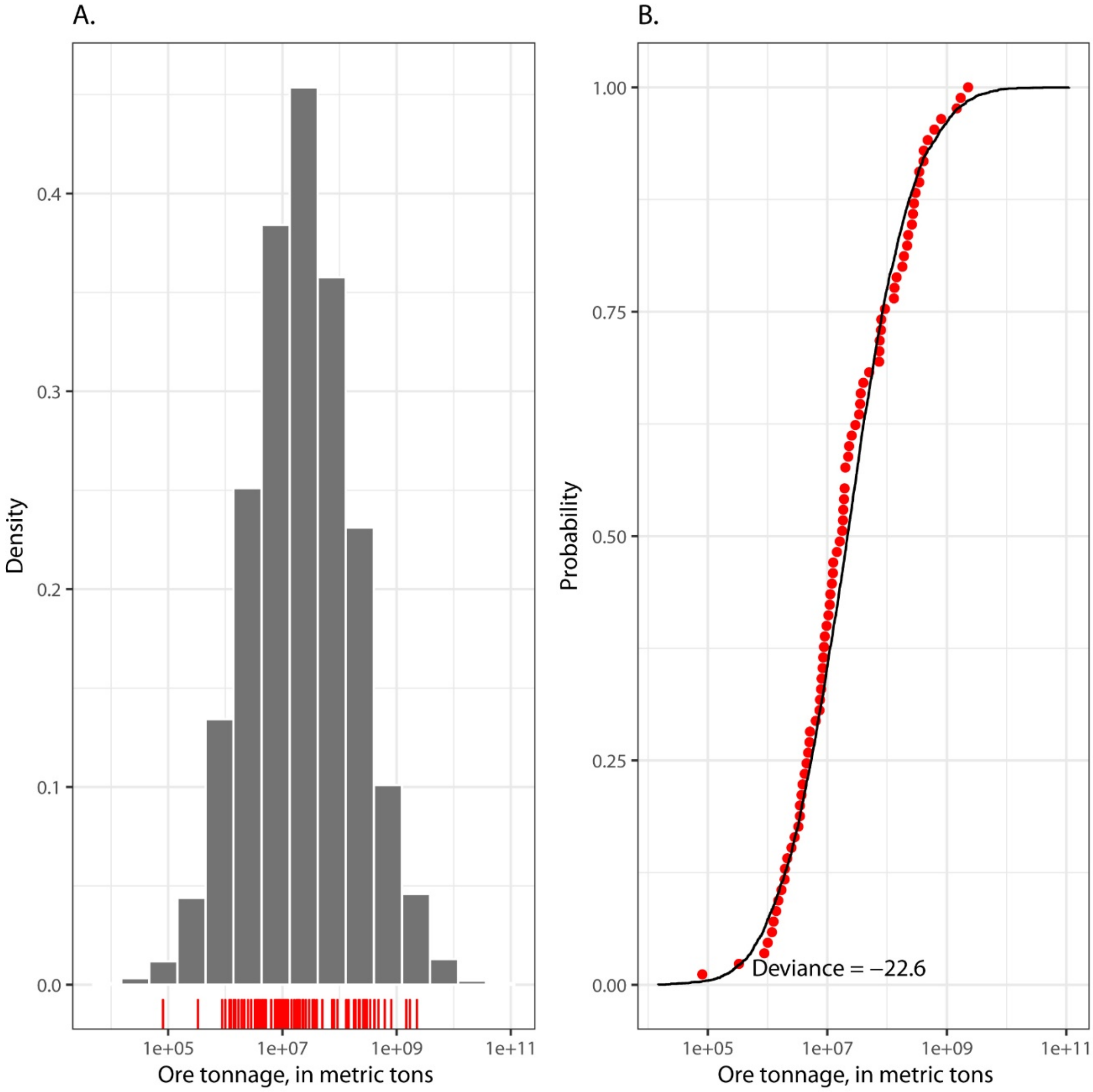

Figure 29. Plot of the estimated ore tonnage or metal tonnage pdf and data for 85 epithermal gold (-silver) deposits derived from the compilation in John et al. (2018).

7.2. Breiðdalur

The permissive tract of the Breiðdalur central volcano extends over an area of 83 km^2.

Undiscovered deposits (negative binomial data)

The undiscovered deposits tool estimates a probability mass function (pmf) for the number of undiscovered deposits that can exist within a permissive tract. The tool provides summary statistics and plots of the input data and estimated probability distribution, and saves the distribution probability mass function for use in Monte Carlo simulation. The tool is based on and uses the R functions of the USGS software MapMark4 (Ellefsen, 2017a, b; Shapiro, 2018) and Eminers (Root et al., 1992; Duval, 2012). The algorithm used by the MARK3 process is given in Appendix 2 of Singer and Menzie (2010).
The probability mass functions (pmf) is estimated based on negative binomial calculation. For negative binomial probability mass function calculation, the estimated numbers for each expert are used as input.
Table 6 provides the estimates for the number of undiscovered epithermal gold deposits in the permissive tract of the Breiðdalur central volcano. Table 7 shows summary of probability mass functions, number of undiscovered deposits for the Breiðdalur central volcano.
Figure 30 shows a plot of the estimated probability mass functions for the Breiðdalur central volcano. For the negative binomial option, the corresponding cumulative distribution function is also plotted together with the expert estimates.
The estimation for undiscovered deposits can be related to the limited exploration history of the Breiðdalur central volcano, as well the lack of any gold showing in the permissive tract. The lack of any gold anomaly may also be related to the erosional level within the Breiðdalur central volcano of about 1000 to 1500 m. Nevertheless, the geological conditions of a well-developed alteration aureole within the Breiðdalur central volcano are favorable for gold deposits.

Table 6. Estimates for the number of undiscovered epithermal gold deposits in the permissive tract of the Breiðdalur central volcano. N90, N50, N10: estimated number of undiscovered deposits associated with the 90th, 50th and 10th percentiles.

Expert	Weight	N90	N50	N10
GOF	1	0	0	1
HF	1	0	0	1
VH	1	0	0	1
TBW	1	0	0	1
BGR	1	0	0	1
GME	1	0	0	1
TB	0.5	0	0	4

This activity has received funding from the European Institute of Innovation and Technology (EIT), a body of the European Union, under the Horizon 2020, the EU Framework Programme for Research and Innovation

Table 7. Summary of probability mass functions, number of undiscovered deposits for the Breiðdalur central volcano.

Type	negative binomial
Mean	0.135
Variance	0.144
St. Dev.	0.379
Mode	0
Smallest N deposits in pmf	0
Largest N deposits in pmf	3
Inform. entropy	0.413

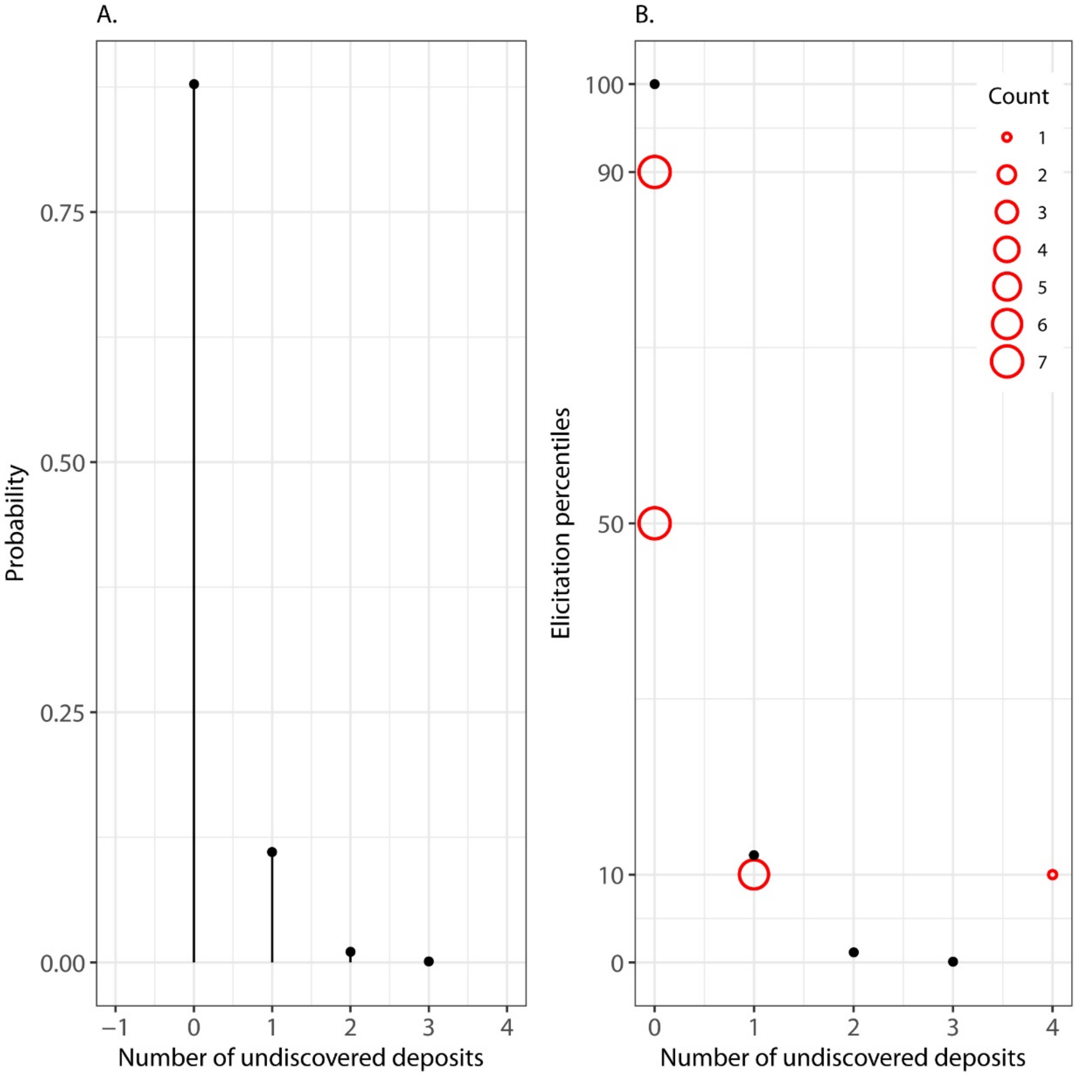

Figure 30. Plot of the estimated probability mass functions for the Breiðdalur central volcano. For the negative binomial option, the corresponding cumulative distribution function is also plotted together with the expert estimates.

This activity has received funding from the European Institute of Innovation and Technology (EIT), a body of the European Union, under the Horizon 2020, the EU Framework Programme for Research and Innovation

Monte Carlo Simulation

The Monte Carlo simulation tool produces a probabilistic estimate of the amount of undiscovered mineral resources within a permissive tract. The tool provides summary statistics and plots of the estimated metal endowments. The tool is based on and uses the R functions of the USGS software MapMark4 (Ellefsen, 2017a,b; Shapiro, 2018).

The tool uses the probability mass function estimated for the number of undiscovered deposits within a permissive tract by the Undiscovered deposits tool together with the probability density functions estimated for ore tonnage and metal grades, or for metal tonnage, by the Grade-tonnage model tool. It creates a large number (default 20,000 simulation rounds) of simulated undiscovered deposits and calculates their metal contents.

Table 8 shows the summary of the probability density functions for the total ore and resource tonnages in all undiscovered deposits within the permissive tract of the Breiðdalur central volcano. Table 9 provides a comparison between statistics estimated from the multivariate probability density functions and statistics from analytic formulas for the permissive tract of the Breiðdalur central volcano. Figure 31 shows the cumulative frequency distributions of simulated undiscovered resources in epithermal deposits in the Breiðdalur tract. Figure 32 shows plots of univariate and bivariate marginal distributions for total ore and metal tonnages in all undiscovered deposits within the permissive tract of the Breiðdalur central volcano.

Table 8. Summary of the probability density functions for the total ore and resource tonnages in all undiscovered deposits within the permissive tract of the Breiðdalur central volcano.

	Quantile							Mean	Probability of	
	0.05	0.1	0.25	0.5	0.75	0.9	0.95		None	Mean or greater
Ore (Mt)	0	0	0	0	0	4.55	42.8	27.1	0.87	0.06
Au (t)	0	0	0	0	0	1.45	17.00	17.40	0.87	0.05

Table 9. Comparison between statistics estimated from the multivariate probability density functions and statistics from analytic formulas for the permissive tract of the Breiðdalur central volcano.

	Mean vectors		Standard deviation vectors		Composite correlation matrix	
	Pdf	Formula	Pdf	Formula	Ore	Au
Ore (Mt)	27.1	24.9	390	522	NA	0.46
Au (t)	17.40	20.40	270	713	0.56	NA

This activity has received funding from the European Institute of Innovation and Technology (EIT), a body of the European Union, under the Horizon 2020, the EU Framework Programme for Research and Innovation

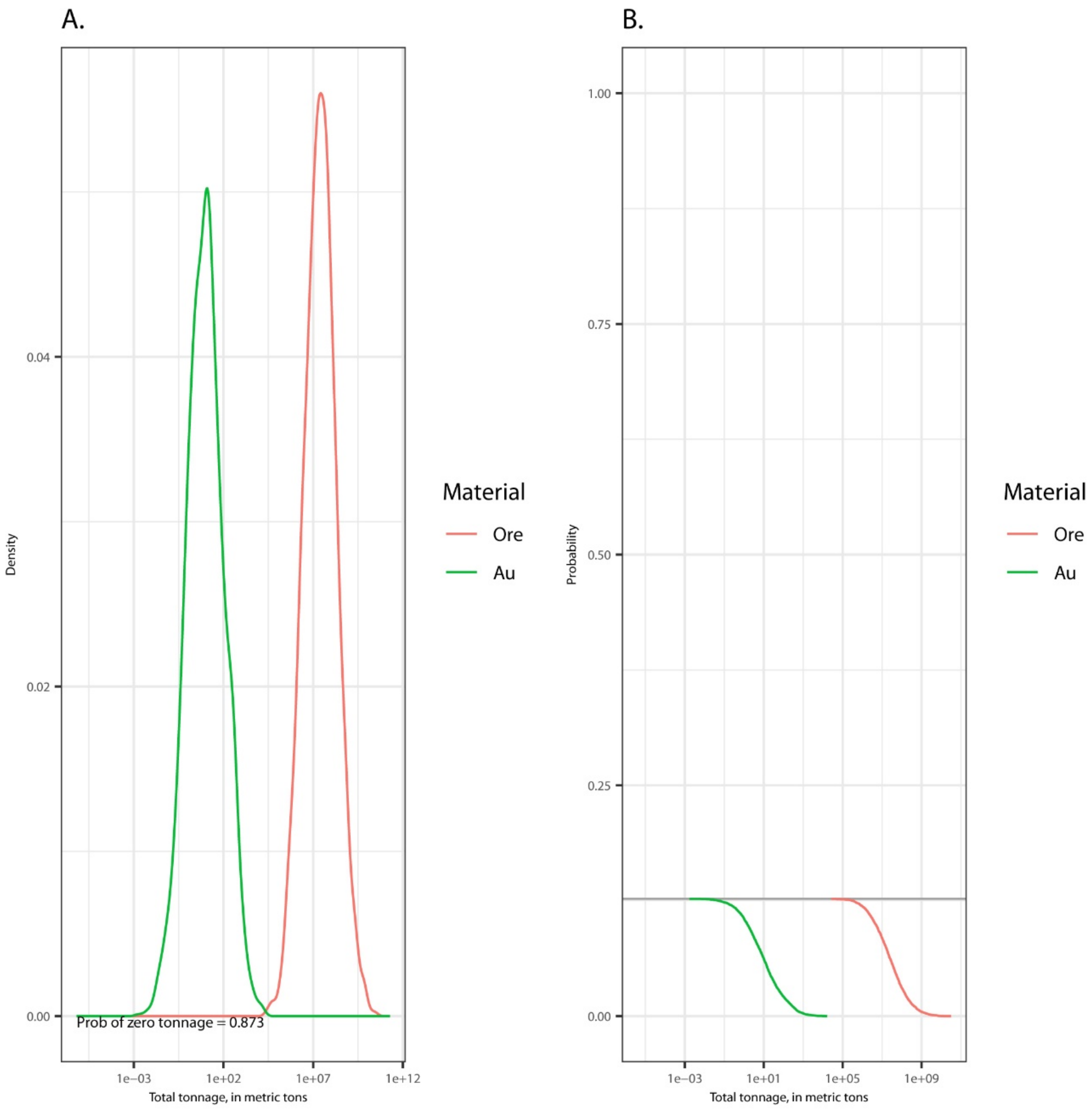

Figure 31. Cumulative frequency distributions of simulated undiscovered resources in epithermal deposits in the Breiðdalur tract.

This activity has received funding from the European Institute of Innovation and Technology (EIT), a body of the European Union, under the Horizon 2020, the EU Framework Programme for Research and Innovation

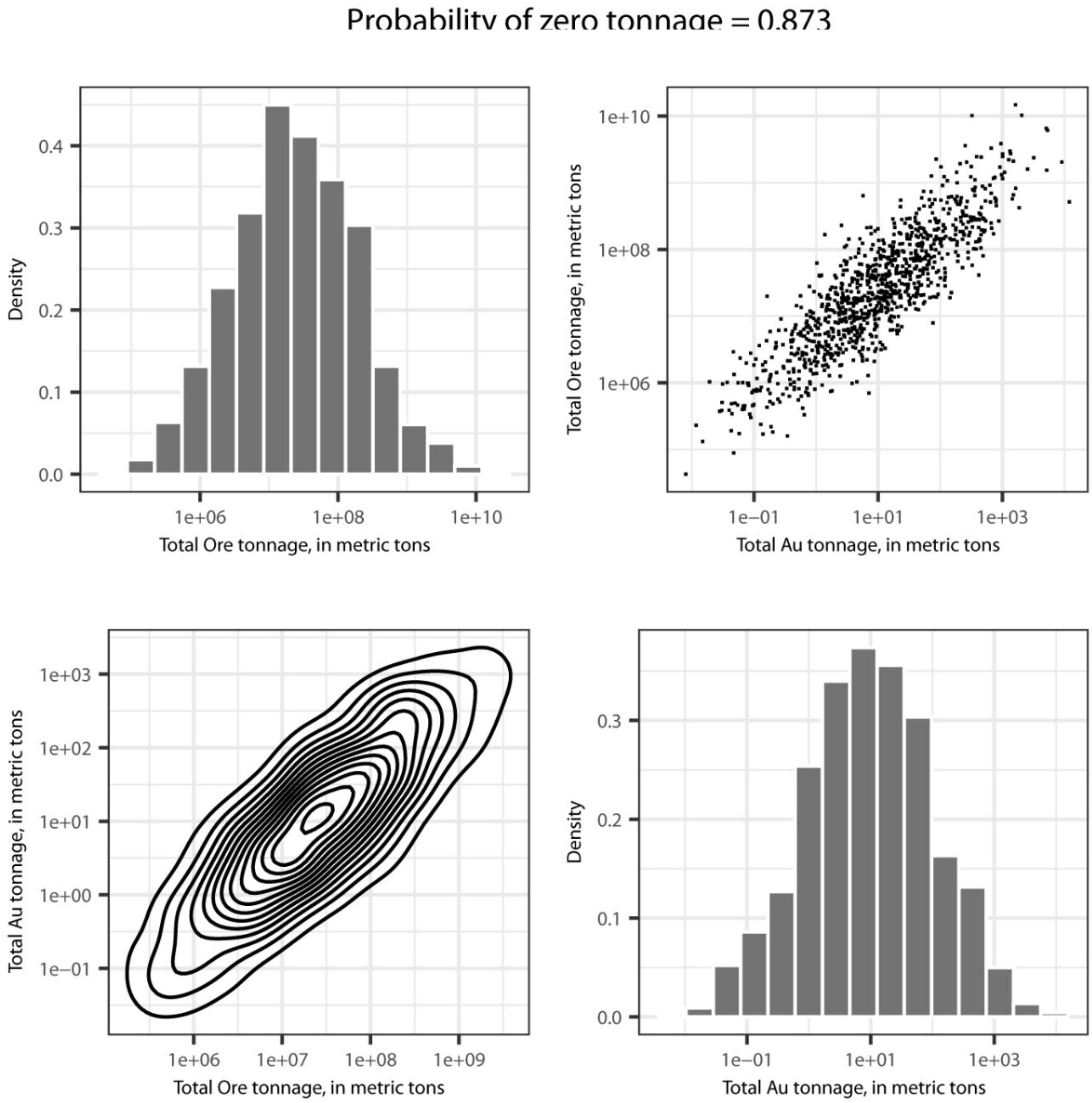

Figure 32. Plots of univariate and bivariate marginal distributions for total ore and metal tonnages in all undiscovered deposits within the permissive tract of the Breiðdalur central volcano.

This activity has received funding from the European Institute of Innovation and Technology (EIT), a body of the European Union, under the Horizon 2020, the EU Framework Programme for Research and Innovation

7.3. Hafnarfjall

The permissive tract of the Hafnarfjall central volcano extends over an area of 222 km^2.

Undiscovered deposits (negative binomial data)

Table 10 provides the estimates for the number of undiscovered epithermal gold deposits in the permissive tract of the Hafnarfjall central volcano. Table 11 shows the summary of probability mass functions, number of undiscovered deposits for the Hafnarfjall central volcano.
Figure 33 shows a plot of the estimated probability mass functions for the Hafnarfjall central volcano. For the negative binomial option, the corresponding cumulative distribution function is also plotted together with the expert estimates.

Table 10. Estimates for the number of undiscovered epithermal gold deposits in the permissive tract of the Hafnarfjall central volcano. N90, N50, N10: estimated number of undiscovered deposits associated with the 90th, 50th and 10th percentiles.

Expert	Weight	N90	N50	N10
GOF	1	0	2	4
HF	1	0	1	1
VH	1	0	0	1
TBW	1	0	0	1
BGR	1	0	1	2
GME	1	0	0	1
TB	0.5	1	2	5

Table 11. Summary of probability mass functions, number of undiscovered deposits for the Hafnarfjall central volcano.

Type	negative binomial
Mean	0.134
Variance	0.143
St. Dev.	0.378
Mode	0
Smallest N deposits in pmf	0
Largest N deposits in pmf	3
Inform. entropy	0.410

The estimation for undiscovered deposits can be related to the limited exploration history of the Hafnarfjall central volcano, as well the lack of any gold showing in the permissive tract. Nevertheless, the geological conditions of a well-developed alteration aureole within the Hafnarfjall central volcano are favorable for gold deposits.

This activity has received funding from the European Institute of Innovation and Technology (EIT), a body of the European Union, under the Horizon 2020, the EU Framework Programme for Research and Innovation

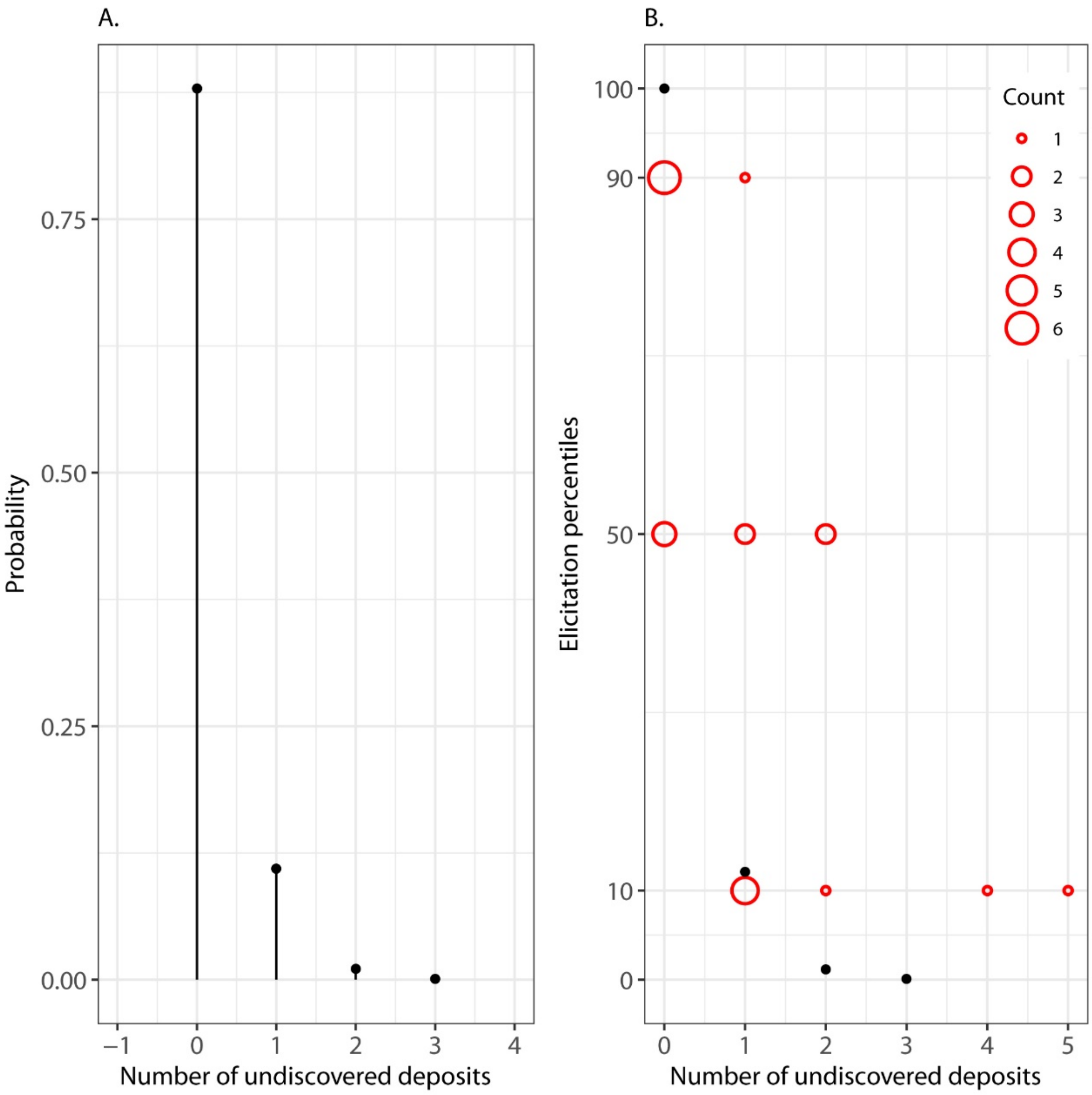

Figure 33. Plot of the estimated probability mass functions for the Hafnarfjall central volcano. For the negative binomial option, the corresponding cumulative distribution function is also plotted together with the expert estimates.

Monte Carlo Simulation

Table 12 shows the summary of the probability density functions for the total ore and resource tonnages in all undiscovered deposits within the permissive tract of the Hafnarfjall central volcano. Table 13 provides a comparison between statistics estimated from the multivariate probability density functions and statistics from analytic formulas for the permissive tract of the

This activity has received funding from the European Institute of Innovation and Technology (EIT), a body of the European Union, under the Horizon 2020, the EU Framework Programme for Research and Innovation

Hafnarfjall central volcano. Figure 34 shows the cumulative frequency distributions of simulated undiscovered resources in epithermal deposits in the Hafnarfjall tract. Figure 35 shows plots of univariate and bivariate marginal distributions for total ore and metal tonnages in all undiscovered deposits within the permissive tract of the Hafnarfjall central volcano.

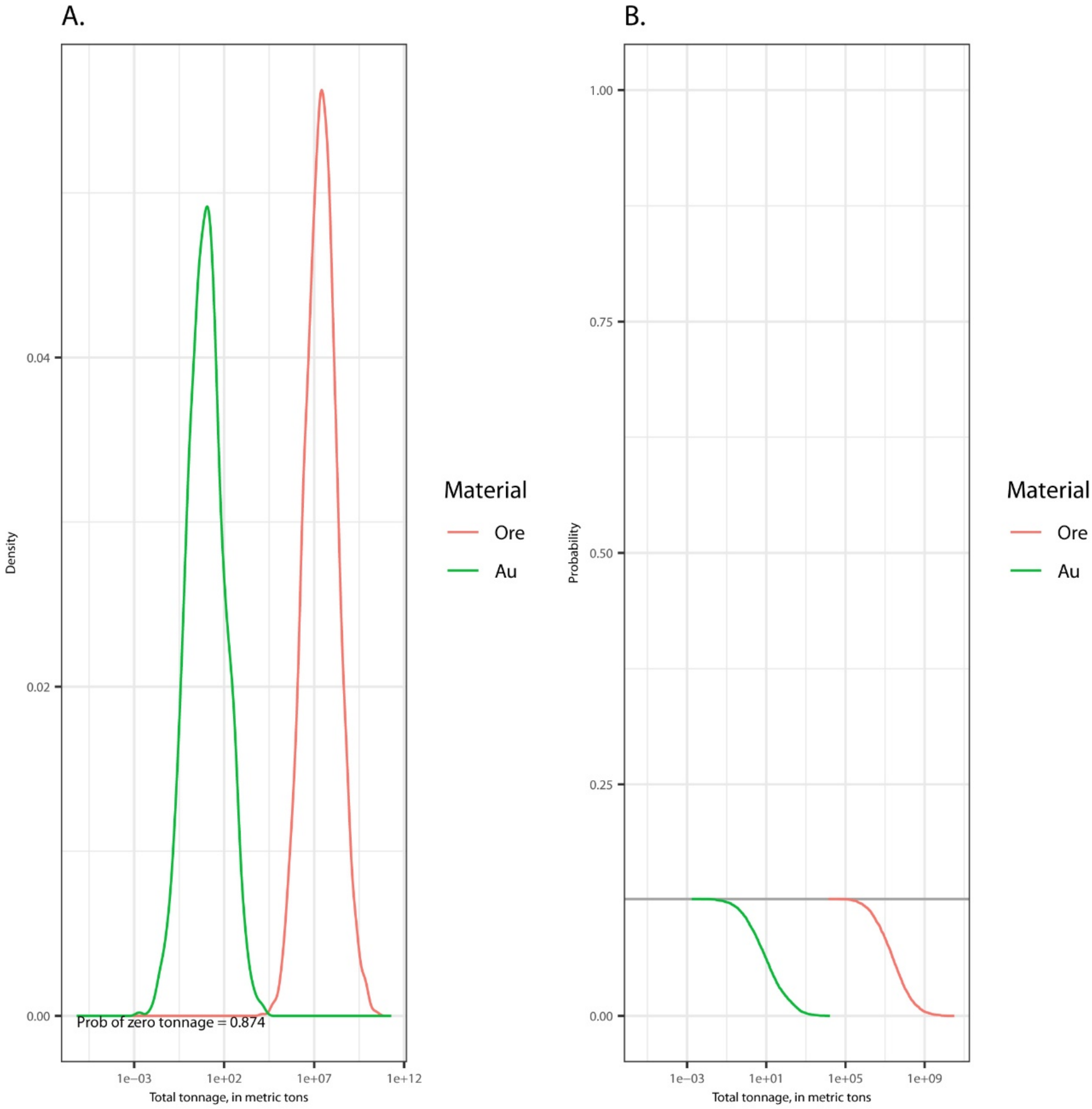

Figure 34. Cumulative frequency distributions of simulated undiscovered resources in epithermal deposits in the Hafnarfjall tract.

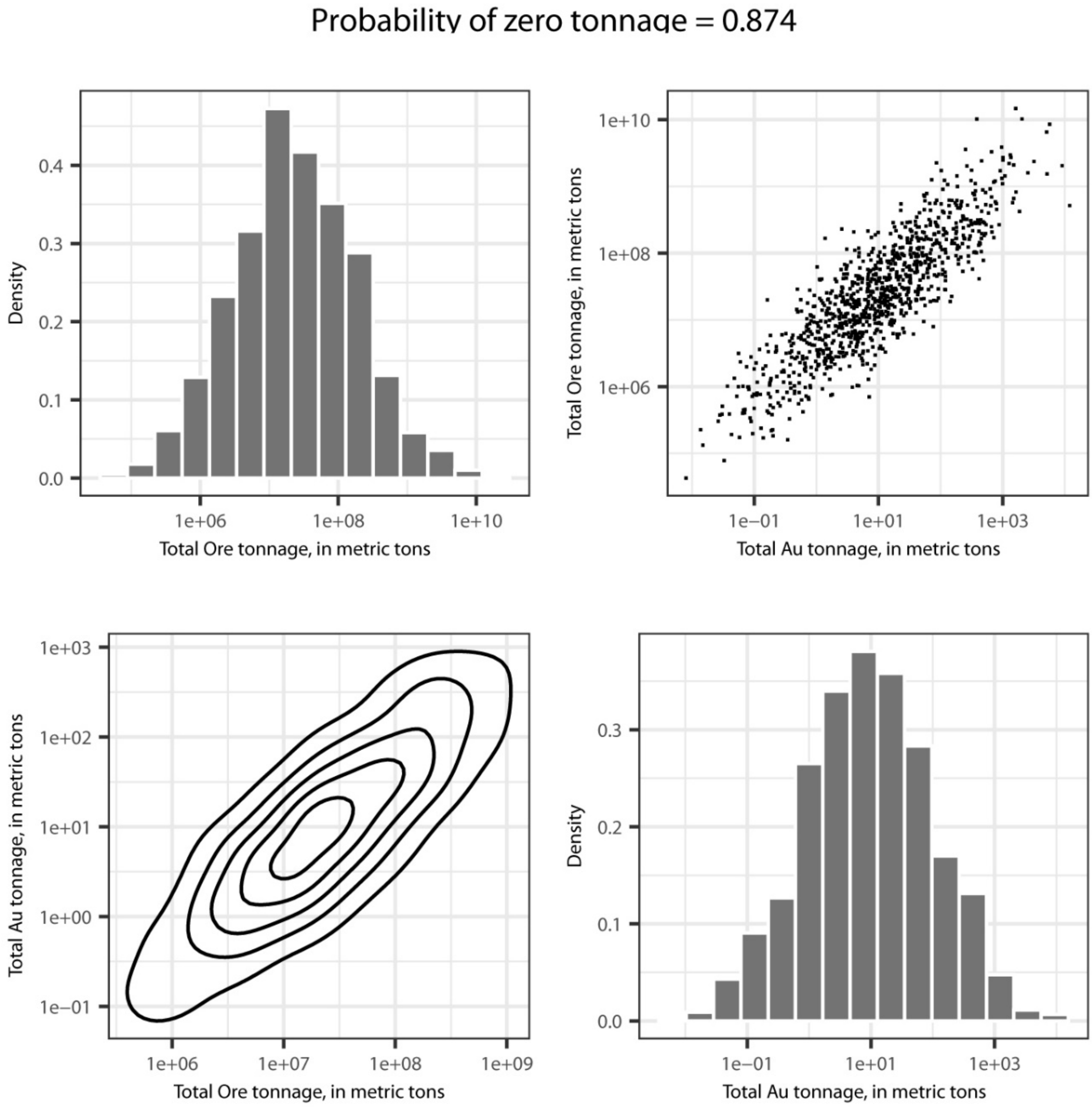

Figure 35. Plots of univariate and bivariate marginal distributions for total ore and metal tonnages in all undiscovered deposits within the permissive tract of the Hafnarfjall central volcano.

This activity has received funding from the European Institute of Innovation and Technology (EIT), a body of the European Union, under the Horizon 2020, the EU Framework Programme for Research and Innovation

Table 12. Summary of the probability density functions for the total ore and resource tonnages in all undiscovered deposits within the permissive tract of the Hafnarfjall central volcano.

	Quantile							Mean	Probability of	
	0.05	0.1	0.25	0.5	0.75	0.9	0.95		None	Mean or greater
Ore (Mt)	0	0	0	0	0	4.32	42	27	0.87	0.06
Au (t)	0	0	0	0	0	1.37	16.80	17.40	0.87	0.05

Table 13. Comparison between statistics estimated from the multivariate probability density functions and statistics from analytic formulas for the permissive tract of the Hafnarfjall central volcano

	Mean vectors		Standard deviation vectors		Composite correlation matrix	
	Pdf	Formula	Pdf	Formula	Ore	Au
Ore (Mt)	27	24.7	393	520	NA	0.46
Au (t)	17.40	20.20	270	710	0.56	NA

7.4. Kjarlarnes/Stardalur

The permissive tract of the Kjarlarnes/Stardalur central volcano extends over an area of 270 km^2.

Undiscovered deposits (negative binomial data)

Table 14 provides the estimates for the number of undiscovered epithermal gold deposits in the permissive tract of the Kjarlarnes/Stardalur central volcano. In contrast to the previous two permissive tracts the estimated for undiscovered gold deposits Kjarlarnes/Stardalur central volcano are significant higher and the experts are more confident. This can directly be related to the two prospect areas Mogilsá and Þormóðsdalur that are part of this permissive.
Table 15 shows Summary of probability mass functions, number of undiscovered deposits for the Kjarlarnes/Stardalur central volcano.
Figure 36 shows a plot of the estimated probability mass functions for the Kjarlarnes/Stardalur central volcano. For the negative binomial option, the corresponding cumulative distribution function is also plotted together with the expert estimates.

This activity has received funding from the European Institute of Innovation and Technology (EIT), a body of the European Union, under the Horizon 2020, the EU Framework Programme for Research and Innovation

Table 14. Estimates for the number of undiscovered epithermal gold deposits in the permissive tract of the Kjarlarnes/Stardalur central volcano. N90, N50, N10: estimated number of undiscovered deposits associated with the 90th, 50th and 10th percentiles.

Expert	Weight	N90	N50	N10
GOF	1	1	2	3
HF	1	2	2	2
VH	1	0	0	2
TBW	1	0	1	2
BGR	1	1	2	4
GME	1	0	1	2
TB	0.5	2	4	10

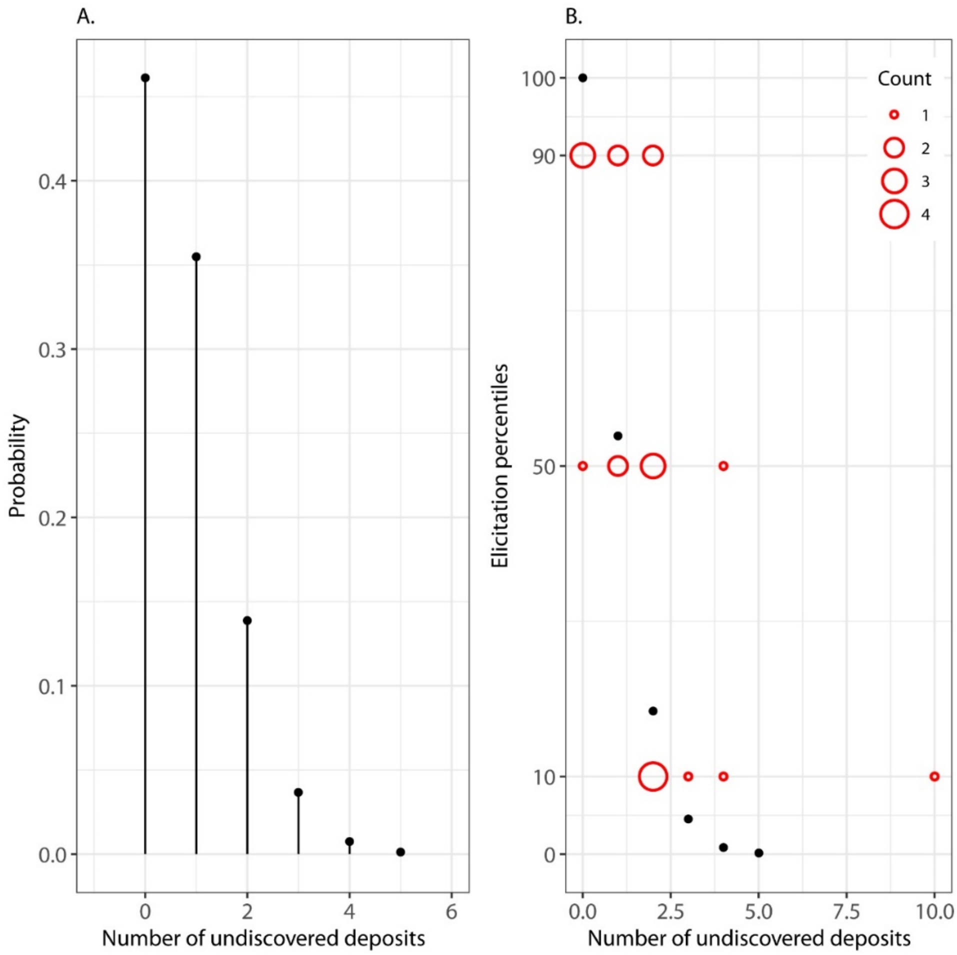

Figure 36. Plot of the estimated probability mass functions for the Kjarlarnes/Stardalur central volcano. For the negative binomial option, the corresponding cumulative distribution function is also plotted together with the expert estimates.

This activity has received funding from the European Institute of Innovation and Technology (EIT), a body of the European Union, under the Horizon 2020, the EU Framework Programme for Research and Innovation

In contrast to the previous two permissive tracts the estimated for undiscovered gold deposits Kjarlarnes/Stardalur central volcano are significant higher and the experts are more confident. This can directly be related to the two prospect areas Mogilsá and Þormóðsdalur that are part of this permissive.

Table 15. Summary of probability mass functions, number of undiscovered deposits for the Kjarlanes/Stardalur central volcano.

Type	negative binomial
Mean	0.778
Variance	0.784
St. Dev.	0.885
Mode	0
Smallest N deposits in pmf	0
Largest N deposits in pmf	5
Inform. entropy	1.165

Monte Carlo Simulation

Table 16shows the summary of the probability density functions for the total ore and resource tonnages in all undiscovered deposits within the permissive tract of the Kjarlarnes/Stardalur central volcano. Table 17 provides a comparison between statistics estimated from the multivariate probability density functions and statistics from analytic formulas for the permissive tract of the Kjarlarnes/Stardalur central volcano. Figure 37 shows the cumulative frequency distributions of simulated undiscovered resources in epithermal deposits in the Kjarlarnes/Stardalur tract. Figure 38 shows plots of univariate and bivariate marginal distributions for total ore and metal tonnages in all undiscovered deposits within the permissive tract of the Kjarlarnes/Stardalur central volcano.

Table 16. Summary of the probability density functions for the total ore and resource tonnages in all undiscovered deposits within the permissive tract of the Kjarlarnes/Stardalur central volcano.

	Quantile							Quantile	Probability of	
	0.05	0.1	0.25	0.5	0.75	0.9	0.95		None	Mean or greater
Ore (Mt)	0	0	0	1.36	45.4	240	558	143	0.47	0.14
Au (t)	0	0	0	0.35	19.1	129	354	106	0.47	0.11

This activity has received funding from the European Institute of Innovation and Technology (EIT), a body of the European Union, under the Horizon 2020, the EU Framework Programme for Research and Innovation

Table 17. Comparison between statistics estimated from the multivariate probability density functions and statistics from analytic formulas for the permissive tract of the Kjarlarnes/Stardalur central volcano.

	Mean vectors		Standard deviation vectors		Composite correlation matrix	
	Pdf	Formula	Pdf	Formula	Ore	Au
Ore (Mt)	143	144	914	1250	NA	0.54
Au (t)	106	118	843	1710	0.56	NA

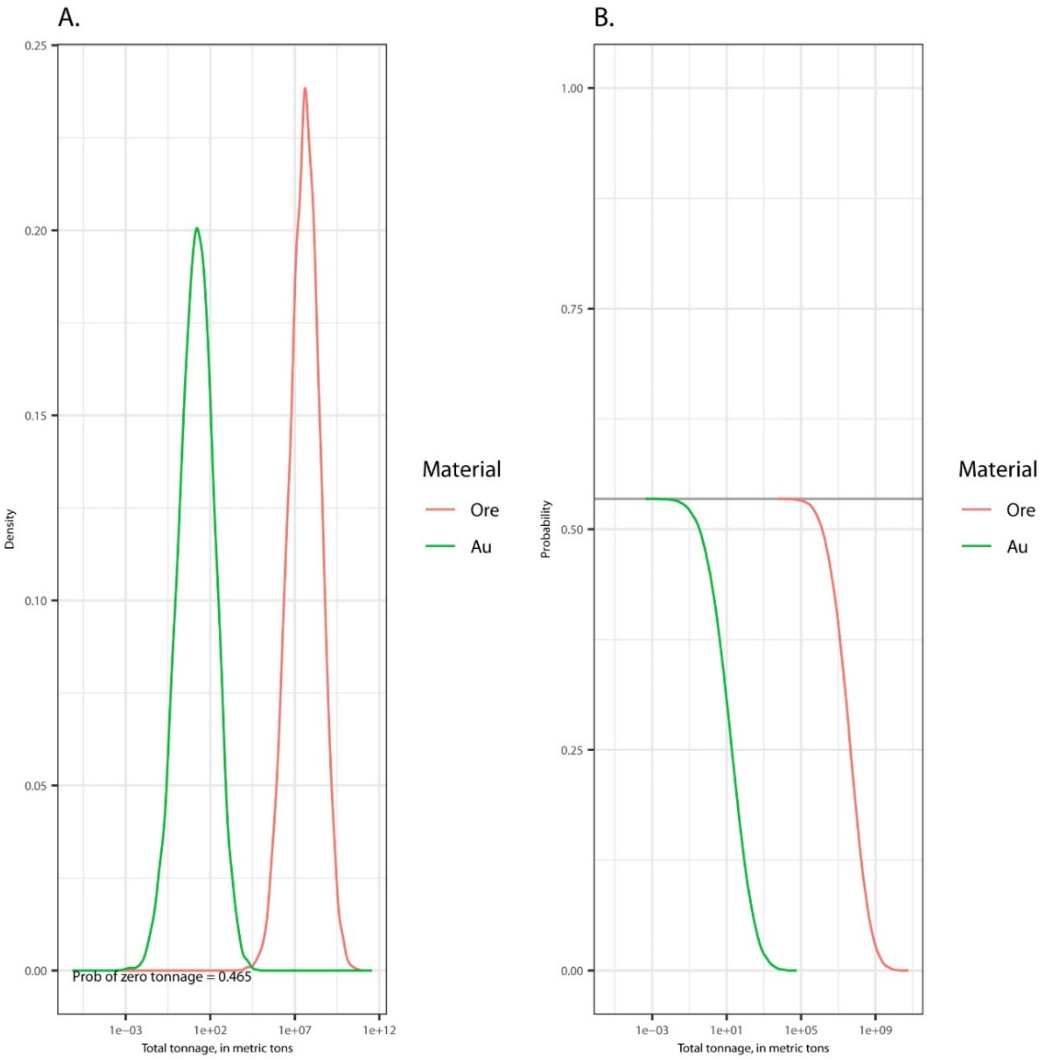

Figure 37. Cumulative frequency distributions of simulated undiscovered resources in epithermal deposits in the Kjarlarnes/Stadalur tract.

This activity has received funding from the European Institute of Innovation and Technology (EIT), a body of the European Union, under the Horizon 2020, the EU Framework Programme for Research and Innovation

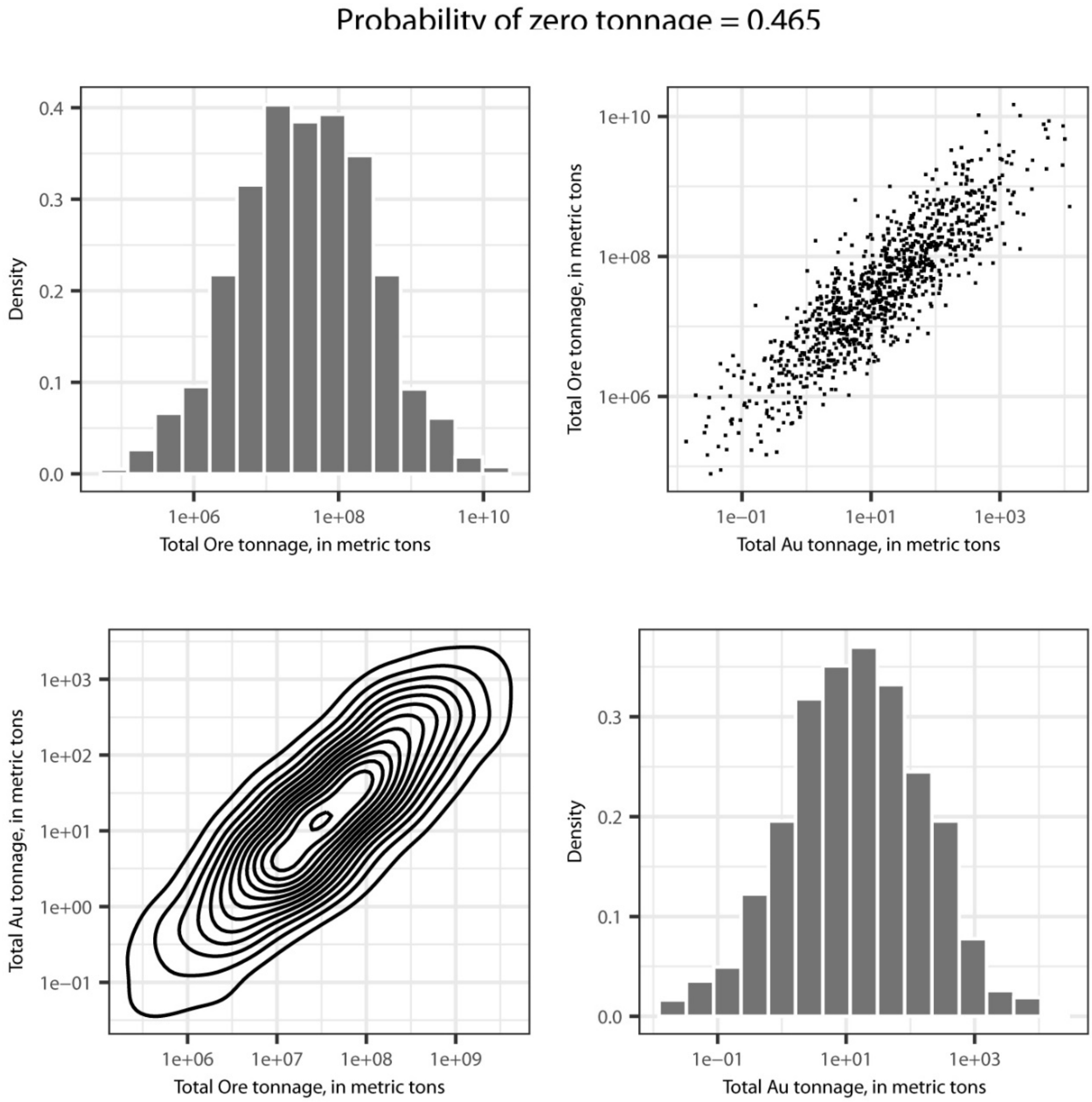

Figure 38. Plots of univariate and bivariate marginal distributions for total ore and metal tonnages in all undiscovered deposits within the permissive tract of the Kjarlarnes/Stardalur central volcano.

This activity has received funding from the European Institute of Innovation and Technology (EIT), a body of the European Union, under the Horizon 2020, the EU Framework Programme for Research and Innovation

7.5. Summary

The assessed potential of epithermal gold for selected permissive tracts in Iceland is very limited. The assessment results can be summarized as following for the three permissive tracts.
The Breiðdalur tract covers an area of 83 km^2. The expected number of undiscovered deposits within the delineated permissive tracts is 0.135 (mean estimate), and the undiscovered deposits are estimated to contain, with 50% probability, no gold. For a probability of 10%, it contains at least 1.45 t of gold. The Hafnarfjall tract covers an area of 222 km^2. The expected number of undiscovered deposits within the delineated permissive tracts is 0.134 (mean estimate), and the undiscovered deposits are estimated to contain, with 50% probability, no gold. For a probability of 10%, it contains at least 1.37 t of gold. The Kjarlarnes/Stardalur tract covers an area of 270 km^2. The expected number of undiscovered deposits within the delineated permissive tracts is 0.778 (mean estimate), and the undiscovered deposits are estimated to contain, with 50% probability, contains at least 0.35 t of gold. For a probability of 10%, it contains at least 129 t of gold.
The low estimated can be related to the limited exploration history as well as the lack of a completed ore formation model. For example, for the Kjarlarnes/Stardalur tract the estimated are higher as the appearance of gold as mineral resource, which gives indication of for possible deposits.
The grade-tonnage model should be interpreted carefully. The adapted grade-tonnage model includes epithermal gold deposits from a worldwide database. Those deposits are hosted within various tectonic settings and show a general large spread in grade and tonnage, The fact that no existing deposits appear within the study area, as well as the lack of comparable geological setting that hosts an epithermal gold deposit indicate a quite high uncertainty.
In general, the estimated epithermal gold in Iceland is quite gold. However, the estimated may change once more exploration data exists and the ore formation model has been elaborated further. This includes better understanding chemical and mineralogical vectors and information on preferred structural traps.

This activity has received funding from the European Institute of Innovation and Technology (EIT), a body of the European Union, under the Horizon 2020, the EU Framework Programme for Research and Innovation

8. Reference

Arnórsson, S., Axelsson, G. and Sæmundsson, K. (2008). *Geothermal systems in Iceland*. Jökull, 58, 269-302.

Askew, R.A. (2020). Breiðdalur *Central Volcano. What came first: The Central Volcano or The Fissure Swarm?* PhD Thesis, University of Iceland, Reykjavík, Iceland, 177 pp.

Barton, P.B. (1993). *Problems and opportunities for mineral deposit models*. In: Kirkham, R.V., Sinclair, W. D., Thorpe, R.I. and Duke, J.M. (Eds.). Mineral deposit modelling. Geological Association of Canada, Special Paper 40, 7-13.

Browning, J. and Gudmundsson, A. (2015). *Caldera faults capture and deflect inclined sheets: an alternative mechanism of ring dike formation.* Bulletin of Volcanology, 77, 1-13.

Chorlton, L., Laramee, R., Sinclair, D. and Hillary, E. (2007). *Data needs and availability. Digital inventory and mineral deposit geology.* In: Briskey, J.A. and Schulz, K.J. (Eds). Proceedings for a Workshop on Deposit Modeling, Mineral Resources Assessment, and Their Role in Sustainable Development, 31st International Geological Congress, Rio de Janeiro, Brazil, August 18–19, 2000. U.S. Geological Survey, Circular 1294, 19-28.

Committee for Mineral Reserves International Reporting Standards (2013). *International Reporting Template for the Public Reporting of Exploration Results, Mineral Resources and Mineral Reserves*. 41 pp.

Cooke, D.R. and Simmons, S.F. (2000). *Characteristics and genesis of epithermal gold deposits.* Society of Economic Geologists Reviews, 13, 221-244.

Corbett, G. (2004). *Comments on the prospectivity of the Tyr project, Iceland for epithermal Au-Ag mineralisation*. Sidney, Corbett Geological Services, 22 pp.

Duval, J.S. (2012). *Version 3.0 of EMINERS – Economic Mineral Resource Simulator*. U.S. Geological Survey, Open-File Report 2004-1344. [Electronic resource]. Available only at http://pubs.usgs.gov/of/2004/1344.

Einaudi, M.T., Hedenquist, J.W. and Inan, E. (2003*). Sulfidation state of hydrothermal fluids - The porphyry-epithermal transition and beyond.* In: Simmons, S.F. and Graham, I.J. (Eds.). Volcanic, geothermal and ore-forming fluids: Rulers and witnesses of processes within the Earth. Special Publication 10, Chapter: 15, Society of Economic Geologists, 285-313.

Ellefsen, K.J. (2017a). *User's guide for MapMark4—An R package for the probability calculations in three-part mineral resource assessments*. U.S. Geological Survey Techniques and Methods. Book 7, Chapter C14, 23 pp.

Ellefsen, K.J. (2017b). *Probability calculations for three-part mineral resource assessments*. U.S. Geological Survey Techniques and Methods. Book 7, chapter C15, 14 pp.

This activity has received funding from the European Institute of Innovation and Technology (EIT), a body of the European Union, under the Horizon 2020, the EU Framework Programme for Research and Innovation

Fleming, A., Nyman, M. and Histed, R. (2006). *Technical report on a core drilling program at the Þormóðsdalur gold prospect and other exploration by Melmi ehf, Iceland 2006.* Husavik, Melmi report, 78 pp.

Franzson, H, (1978), Structure and petrochemistry of the Hafnarfjall_Skardsheidi central volcano and the surrounding basalt succession, W-Iceland. PhD thesis, University of Edinburgh Edinburgh, Scotland, 264 pp.

Franzson, H. and Fridleifsson, G.O. (1993). *Exploration for gold: results of third year´s survey.* Reykjavik, Malmis report, 55 pp.

Franzson, H., Fridleifsson, G.O., Tomasson, Th., Jonasson, H. and Fridleifsson, I.B. (1992). *Exploration for gold and other precious metals: results of second year of exploration.* Reykjavik, Malmis report, 51 pp.

Franzson, H., Fridleifsson, G.O., Bjarnason, B. and Jonasson, H. (1995). Epithermal gold exploration in Iceland. In: Kharaka, Y.K. and Chudaev, O.V. (Edss). Proceedings of the 8th International Symposium on Water-Rock Interaction, Vladivostok, Russia, 15-19 August, 1995, 671-674.

Franzson, H., Fridleifsson, G.O., Bjarnason, B. and Jonasson, H. (1997). *Gold exploration in Iceland*. Geological Society of Iceland, Spring Meeting, Reykjavik, 22 April 1997, 26-28.

Franzson, H., Fridleifsson, G.O. and Jonasson, H, (2013). *Gold exploration in Iceland*. Proceedings, 12th SGA Biennial Meeting, Uppsala, Sweden, 12-15 August 2013, 1862-1865.

Franzson H., Róbertsdóttir B.G., Friðleifsson G.Ó. and Harðardóttir V. (2016*). Chapter 4 Iceland. In: Mineral Resources in the Arctic. In:* Boyd R., Bjerkgård, T., Nordahl, B. and Schiellerup, H. (Eds.). NGU – Geological Survey of Norway, 191-207.

Fridleifsson, I.B. (1973). *Petrology and structure of the Esja Quaternary volcanic region, Southwest Iceland.* PhD thesis, University of Oxford, Oxford, England, 208 pp.

Fridleifsson, G.O., *Franzson, H., Bjarnason, B., Jónasson, H., Ros, F., Flavelle, A., Miller, P. and Karajas, J. (1997). Saga gullleitar í Þormóðsdal (history of gold exploration in Þormóðsdalur). Geological Society of Iceland, Spring Meeting, 23-25.*

Gautneb. H., Gudmundsson. A. and Oskarsson, N. (1989). Structure, petrochemistry and evolution of a sheet swarm in an Icelandic central volcano. Geological Magazine, 126,659-673.

Geirsson, K. (1993). *Pétrologie d'une série tholéiitique complète: le volcan central de Fagridalur*. PhD thesis, Université Pierre et Marie Curie, Paris VI, France, 217 pp.

Grant, H.L.J., Hannington, M.D., Hardardóttir, V., Fuchs, S.H. and Schumann, D. (2020*). Trace metal distributions in sulfide scales of the seawater-dominated Reykjanes geothermal system: Constraints on sub-seafloor hydrothermal mineralizing processes and metal fluxes.* Ore Geology Reviews, 116, 103145.

Gústafsson, L.E. (1992). *Geology and petrography of the Dyrfjöll Central Volcano, eastern Iceland.* Selbstverlag Fachbereich Geowissenschaften, FU Berlin,138, 98 pp.

This activity has received funding from the European Institute of Innovation and Technology (EIT), a body of the European Union, under the Horizon 2020, the EU Framework Programme for Research and Innovation

Hannington, M., Harðardóttir, V., Garbe-Schönberg D. and Brown K.L (2016). *Gold enrichment in active geothermal systems by accumulating colloidal suspensions.* Nature Geosciences 9, 299-302.

Hardardottir, V., Brown, K.L., Fridriksson, Th., Hedenquist, J.W., Hannington, M.D. and Thorhallsson, S. (2009). *Metals in deep liquid of the Reykjanes geothermal system, Southwest Iceland: Implications for the composition of seafloor black smoker fluids.* Geology, 37, 1103-1106.

Hedenquist, J.W., Arribas, A.R. and Gonzalez-Urien, E. (2000). *Exploration for epithermal gold deposits.* In Hagemann, S.G. and Brown, P.E. (Eds.). Gold in 2000: Society of Economic Geologists, Reviews in Economic Geology, 13, 245-277.

Henley, R.W. and Ellis, A.J. (1983). *Geothermal systems, ancient and modern—A geochemical review.* Earth-Science Reviews, 19, 1-50.

Hjartarson, Á. and Sæmundsson, K. (2014). *Geological Map of Iceland. Bedrock. 1:600 000.* Iceland GeoSurvey.

Jankovic, S. (1970). *Reconnaissance prospection for base-metal mineralization in Southeastern Iceland.* Reykjavik, National Research Council, National Energy Authority & United Nations Technical Assistance report, 56 pp.

John D.A., Vikre P.G., du Bray E.A., Blakely R.J., Fey D.L., Rockwell B.W., Mauk J.L., Anderson E.D. and Graybeal, F.T. (2018). *Descriptive models for epithermal gold-silver deposits.* U.S. Geological Survey Scientific Investigations Report 2010–5070–Q, 247 pp.

Ketilsson, J., Björnsson, A., Sveinbjörnsdóttir, A. E., Pálsson, B., Björnsson, G., Axelsson, G. and Sæmundsson, K. (2010). *Nature of geothermal energy and its sustainable utilisation.* In Icelandic. OS-2010/05, Orkustofnun.

Kousehlar, M., Weisenberger, T. B., Tutti, F. and Mirnejad, H. (2012). *Fluid control on low-temperature mineral formation in volcanic rocks of Kahrizak, Iran.* Geofluids, 12, 295-311.

Kristjánsson, B. (1929). *Um málma á Íslandi (The presence of metals in Iceland).* Vaka, 34 pp.

Kristmannsdóttir, H. (1978*). Alteration of basaltic rocks by hydrothermal activity at 100–300 °C.* In: Mortland, M.M. and Farmer, V.C. (Eds.). Proceedings of the VI International Clay Conference 1978, July 10–14, 1978, Oxford, UK. Elsevier, New York, NY, USA, 277-288.

Lindgren, W. (1928). *Mineral Deposits.* (3rd ed.) New York, McGraw-Hill, 1049 pp.

Lindgren, W. (1933). *Mineral Deposits* (4th ed.) New York, McGraw-Hill, 930 pp.

Mehegan, J.M., Robinson, P.T. and Delaney, J.R. (1982). *Secondary Mineralization and Hydrothermal Alteration in the Reydarfjordur Drill Core, Eastern Iceland.* Journal of Geophysical Research – Solid Earth, 87, B8, 6511-6524.

Nesbitt, B.E., St. Louis, R.M. and Muehlenbachs, K. (1986*). Mobility of gold during hydrothermal alteration of basaltic units.* 5th International Symposium on Water-Rock Interaction, Reykjavik, Iceland, August 8-17, 1986, 401-404.

This activity has received funding from the European Institute of Innovation and Technology (EIT), a body of the European Union, under the Horizon 2020, the EU Framework Programme for Research and Innovation

Neuhoff, P.S., Fridriksson, Th. Arnórsson, S. and Bird, D.K. (1999). *Porosity, evolution and mineral paragenesis during low-grade metamorphism of basaltic lavas at Teigarhorn, eastern Iceland.* American Journal of Science, 299, 467-501.

Oliver, J. (1993). *Geological and geochemical characteristics and exploration potential of epithermal gold mineralization in Western Iceland.* Kamloops BC, Teck Exploration report, 96 pp.

Payne, C.E., Cunningham, F., Peters, K.J., Nielsen, S., Puccioni, E., Wildman, C. and Partington, G.A. (2015). *From 2D to 3D: prospectivity modelling in the Taupo Volcanic Zone, New Zealand.* Ore Geology Reviews, 71, 558–577.

Peach, C.L., Mathez, E.A. and Keays, R.R. (1990). *Sulfide melt-silicate melt distribution coefficients for noble metals and other chalcophile elements as deduced from MORB: Implications for partial melting.* Geochimica et Cosmochimica Acta, 54, 3379-3389.

Rasilainen, K., Eilu, P., Halkoaho, T., Karvinen, A., Kontinen, A., Kousa, J., Lauri, L., Luukas, J., Niiranen, T., Nikander, J., Sipilä, P., Sorjonen-Ward, P., Tiainen, M., Törmänen, T. and Västi, K. (2014). *Quantitative assessment of undiscovered resources in volcanogenic massive sulphide deposits, porphyry copper deposits and Outokumpu-type deposits in Finland.* Geological Survey of Finland, Report of Investigation 208, 60 pp.

Root, D.H., Menzie, W.D. and Scott, W.A. (1992). *Computer Monte Carlo simulation in quantitative resource estimation*. Natural Resources Research 1, 125-138.

Shapiro, J. (2018*). User's guide for MapMark4GUI—A graphical user interface for the MapMark4 R package.* U.S. Geological Survey Techniques and Methods. Book 7, Chapter C18, 19 pp.

Sillitoe, R.H. and Hedenquist, J.W. (2003). *Linkages between volcanotectonic settings, ore fluid compositions, and epithermal precious metal deposits.* Society of Economic Geologists Special Publication, 10, 315-343.

Simmons, S.F., White, N.C. and John, D.A. (2005). *Geological characteristics of epithermal precious and base metal deposits.* Economic Geology 100th Anniversary Volume, 485-522.

Singer, D.A. (1975). *Mineral resource models and the Alaskan Mineral Resource Assessment Program.* In: Vogely, W.A. (Ed.). Mineral materials modelling: a state-of-the-art review. Baltimore: Johns Hopkins University Press, 370–382.

Singer, D.A. (1993). *Basic concepts in three-part quantitative assessments of undiscovered mineral resources.* Nonrenewable Resources, 2, 69-81.

Singer, D.A. (2007). *Estimating Amounts of Undiscovered Mineral Resources.* In: Briskey, J.A. and Schulz, K.J. (Eds.). Proceedings for a Workshop on Deposit Modeling, Mineral Resource Assessment, and Their Role in Sustainable Development, 31st International Geological Congress, Rio de Janeiro, Brazil, August 18–19, 2000. U.S. Geological Survey, Circular 1294, 79–84.

Singer, D.A. and Menzie, W.D. (2010). *Quantitative mineral resource assessments: An integrated approach.* New York: Oxford University Press. 219 pp.

This activity has received funding from the European Institute of Innovation and Technology (EIT), a body of the European Union, under the Horizon 2020, the EU Framework Programme for Research and Innovation

Singer, D.A., Berger, V.I. and Moring, B.C. (2008). *Porphyry Copper Deposits of the World: Database and Grade and Tonnage Models, 2008.* U.S. Geological Survey, Open-File Report 2008-1155. 45 pp.

Taylor, B.E. (2007). *Epithermal gold deposits.* In: Goodfellow, W.D. (Ed.). Mineral Deposits of Canada: A Synthesis of Major Deposit-Types, District Metallogeny, the Evolution of Geological Provinces, and Exploration Methods: Geological Association of Canada, Mineral Deposits Division, Special Publication. 5, 113-139.

Thordarson, Th. (2012). *Outline of Geology of Iceland.* Chapman Conference 2012, 15 pp.

U.S. Bureau of Mines and U.S. Geological Survey (1980). *Principles of a resource/reserve classification for minerals.* U.S. Geological Survey, Circular 831, 5 pp.

U.S. Geological Survey National Mineral Resource Assessment Team (2000). 1998 *Assessment of Undiscovered Deposits of Gold, Silver, Copper, Lead, and Zinc in the United States.* U.S. Geological Survey, Circular 1178, 22 pp.

Walker, G.P. (1960). *Zeolite zones and dike distribution in relation to the structure of the basalts of eastern Iceland.* The Journal of Geology. 68, 515-528.

Walker, G.P. (1963). *The Breiddalur central volcano, eastern Iceland.* Quarterly Journal of the Geological Society, 119, 29-63.

Weisenberger, T. and Selbekk, R.S. (2009). *Multi-stage zeolite facies mineralization in the Hvalfjördur area, Iceland.* International Journal of Earth Sciences. 98, 985-999.

Weisenberger, T.B., Ingimarsson, H., Hersir, G.P. and Flóvenz, Ó.G. (2020). *Cation-Exchange Capacity Distribution within Hydrothermal Systems and Its Relation to the Alteration Mineralogy and Electrical Resistivity.* Energies, 13, 5730.

White N.C. and Hedenquist J.W. (1995). *Epithermal gold deposits: styles, characteristics and exploration.* SEG Newsletter, 23, 9-13.

Zentilli, M., Brooks, R.R., Helgason, J., Ryan, D.E. and Zhang, H. (1985). *The distribution of gold in volcanic rocks of eastern Iceland.* Chemical Geology, 48, 17-28.

This activity has received funding from the European Institute of Innovation and Technology (EIT), a body of the European Union, under the Horizon 2020, the EU Framework Programme for Research and Innovation